Eur. Phys. J. C (2014) 74:3014
DOI 10.1140/epjc/s10052-014-3014-0

THE EUROPEAN PHYSICAL JOURNAL C

Regular Article - Experimental Physics

# Measurement of jet multiplicity distributions in $t\bar{t}$ production in pp collisions at $\sqrt{s} = 7$ TeV

**The CMS Collaboration***

CERN, 1211 Geneva 23, Switzerland

Received: 11 April 2014 / Accepted: 30 July 2014 / Published online: 20 August 2014


**Abstract** The normalised differential top quark-antiquark production cross section is measured as a function of the jet multiplicity in proton-proton collisions at a centre-of-mass energy of 7 TeV at the LHC with the CMS detector. The measurement is performed in both the dilepton and lepton+jets decay channels using data corresponding to an integrated luminosity of 5.0 $\text{fb}^{-1}$. Using a procedure to associate jets to decay products of the top quarks, the differential cross section of the $t\bar{t}$ production is determined as a function of the additional jet multiplicity in the lepton+jets channel. Furthermore, the fraction of events with no additional jets is measured in the dilepton channel, as a function of the threshold on the jet transverse momentum. The measurements are compared with predictions from perturbative quantum chromodynamics and no significant deviations are observed.

## 1 Introduction

Precise measurements of the top quark-antiquark ($t\bar{t}$) production cross section and top-quark properties performed at the CERN Large Hadron Collider (LHC) provide crucial information for testing the predictions of perturbative quantum chromodynamics (QCD) at large energy scales and in processes with multiparticle final states.

About half of the $t\bar{t}$ events are expected to be accompanied by additional hard jets that do not originate from the decay of the $t\bar{t}$ pair ($t\bar{t}$ +jets). In this paper, these jets will be referred to as *additional jets*. These processes typically arise from either initial- or final-state QCD radiation, providing an essential handle to test the validity and completeness of higher-order QCD calculations of processes leading to multijet events. Calculations at next-to-leading order (NLO) are available for $t\bar{t}$ production in association with one [1] or two [2] additional jets. The correct description of $t\bar{t}$ +jets production is important to the overall LHC physics program since it constitutes an important background to processes with multijet final states, such as associated Higgs-boson production with a $t\bar{t}$ pair, with the Higgs boson decaying into a $b\bar{b}$ pair, or final states predicted in supersymmetric theories. Anomalous production of additional jets accompanying a $t\bar{t}$ pair could be a sign of new physics beyond the standard model [3].

This paper presents studies of the $t\bar{t}$ production with additional jets in the final state using data collected in proton-proton (pp) collisions with centre-of-mass energy $\sqrt{s} = 7$ TeV with the Compact Muon Solenoid (CMS) detector [4]. The analysis uses data recorded in 2011, corresponding to a total integrated luminosity of $5.0 \pm 0.1$ $\text{fb}^{-1}$. For the first time, the $t\bar{t}$ cross section is measured differentially as a function of jet multiplicity and characterised both in terms of the total number of jets in the event, as well as the number of additional jets with respect to the leading-order hard-interaction final state. Kinematic properties of the additional jets are also investigated. The results are corrected for detector effects and compared at particle level with theoretical predictions obtained using different Monte Carlo (MC) event generators.

The differential cross sections as a function of jet multiplicity are measured in both the dilepton (ee, $\mu\mu$, and e$\mu$) and $\ell$+jets ($\ell$ = e or $\mu$) channels. For the dilepton channel, data containing two oppositely charged leptons and at least two jets in the final state are used, while for the $\ell$+jets channel, data containing a single isolated lepton and at least three jets are used. Following the analysis strategy applied to the measurement of other $t\bar{t}$ differential cross sections [5], the results are normalised to the inclusive cross section measured in situ, eliminating systematic uncertainties related to the normalisation. Lastly, the fraction of events that do not contain additional jets (*gap fraction*), first measured by ATLAS [6], is determined in the dilepton channel as a function of the threshold on the transverse momentum ($p_{\text{T}}$) of the leading additional jet and of the scalar sum of the $p_{\text{T}}$ of all additional jets.

The measurements are performed in the visible phase space, defined as the kinematic region in which all selected final-state objects are produced within the detector accep-

* e-mail: cms-publication-committee-chair@cern.ch

tance. This avoids additional model uncertainties due to the extrapolation of the measurements into experimentally inaccessible regions of phase space.

The paper is structured as follows. A brief description of the CMS detector is provided in Sect. 2. Section 3 gives a description of the event simulation, followed by details of the object reconstruction and event selection in Sect. 4. A discussion of the sources of systematic uncertainties is given in Sect. 5. The measurement of the differential cross section is presented as a function of the jet multiplicity in Sect. 6 and as a function of the additional jet multiplicity in Sect. 7. The study of the additional jet gap fraction is described in Sect. 8. Finally, a summary is given in Sect. 9.

## 2 The CMS detector

The central feature of the CMS apparatus is a superconducting solenoid, 13 m in length and 6 m in diameter, which provides an axial magnetic field of 3.8 T. The bore of the solenoid is outfitted with various particle detection systems. Charged-particle trajectories are measured with silicon pixel and strip trackers, covering $0 \leq \phi < 2\pi$ in azimuth and $|\eta| < 2.5$ in pseudorapidity, where $\eta$ is defined as $\eta = -\ln[\tan(\theta/2)]$, with $\theta$ being the polar angle of the trajectory of the particle with respect to the anticlockwise-beam direction. A lead tungstate crystal electromagnetic calorimeter (ECAL) and a brass/scintillator hadron calorimeter (HCAL) surround the tracking volume. The calorimetry provides excellent resolution in energy for electrons and hadrons within $|\eta| < 3.0$. Muons are measured up to $|\eta| < 2.4$ using gas-ionisation detectors embedded in the steel flux return yoke outside the solenoid. The detector is nearly hermetic, providing accurate measurements of any imbalance in momentum in the plane transverse to the beam direction. The two-level trigger system selects most interesting final states for further analysis. A detailed description of the CMS detector can be found in Ref. [4].

## 3 Event simulation

The reference simulated $\mathrm{t\bar{t}}$ sample used in the analysis is generated with the MadGraph (v. 5.1.1.0) matrix element generator [7], with up to three additional partons. The generated events are subsequently processed using pythia (v. 6.424) [8] to add parton showering using the MLM prescription [9] for removing the overlap in phase space between the matrix element and the parton shower approaches. The pythia Z2 tune is used to describe the underlying event [10]. The top-quark mass is assumed to be $m_{\mathrm{t}} = 172.5\,\mathrm{GeV}$. The proton structure is described by the CTEQ6L1 [11] parton distribution functions (PDFs).

The MadGraph generator is used to simulate W+jets and $\mathrm{Z}/\gamma^*$+jets production. Single-top-quark events ($s$-, $t$-, and tW-channels) are simulated using powheg (r1380) [12–15]. Diboson (WW, WZ, and ZZ) and QCD multijet events are simulated using pythia.

Additional $\mathrm{t\bar{t}}$ and W+jets MadGraph samples are generated using different choices for the common factorisation and renormalisation scale ($\mu_F^2 = \mu_R^2 = Q^2$) and for the jet-parton matching threshold. These are used to determine the systematic uncertainties due to model uncertainties and for comparisons with the measured distributions. The nominal $Q^2$ scale is defined as $m_{\mathrm{t}}^2 + \sum p_{\mathrm{T}}^2(\mathrm{jet})$. This is varied between $4Q^2$ and $Q^2/4$. For the reference MadGraph sample, a jet-parton matching threshold of 20 GeV is chosen, while for the up and down variations, thresholds of 40 and 10 GeV are used, respectively.

In addition to MadGraph, samples of $\mathrm{t\bar{t}}$ events are generated with powheg and mc@nlo (v. 3.41) [16]. The CTEQ6M [11] PDF set is used in both cases. Both powheg and mc@nlo match calculations to full NLO accuracy with parton shower MC generators. For powheg, pythia is chosen for hadronisation and parton shower simulation, with the same Z2 tune utilised for other samples. For mc@nlo, herwig (v. 6.520) [17] with the default tune is used.

For comparison with the measured distributions, the event yields in the simulated samples are normalised to an integrated luminosity of $5.0\,\mathrm{fb}^{-1}$ according to their theoretical cross sections. These are taken from next-to-next-to-leading-order (NNLO) (W+jets and $\mathrm{Z}/\gamma^*$+jets), NLO plus next-to-next-to-leading-log (NNLL) (single-top-quark $s$- [18], $t$- [19] and tW-channels [20]), NLO (diboson [21]), and leading-order (LO) (QCD multijet [8]) calculations. For the simulated $\mathrm{t\bar{t}}$ sample, the full NNLO+NNLL calculation, performed with the Top++ 2.0 program [22], is used. The PDF and $\alpha_S$ uncertainties are estimated using the PDF4LHC prescription [23,24] with the MSTW2008nnlo68cl [25], CT10 NNLO [26,27], and NNPDF2.3 5f FFN [28] PDF sets, and added in quadrature to the scale uncertainty to obtain a $\mathrm{t\bar{t}}$ production cross section of $177.3^{+10.1}_{-10.8}$ pb (for a top-quark mass value of 172.5 GeV).

All generated samples are passed through a full detector simulation using Geant4 [29], and the number of additional pp collisions (pileup) is matched to the real distribution as inferred from data.

## 4 Event reconstruction and selection

The event selection is based on the reconstruction of the $\mathrm{t\bar{t}}$ decay products. The top quark decays almost exclusively into a W boson and a b quark. Only the subsequent decays of one or both W bosons to a charged lepton and a neutrino are considered here. Candidate events are required to contain

the corresponding reconstructed objects: isolated leptons and jets. The requirement of the presence of jets associated with b quarks or antiquarks (b jets) is used to increase the purity of the selected sample. The selection has been optimised independently in each channel to maximise the signal content and background rejection.

### 4.1 Lepton, jet, and missing transverse energy reconstruction

Events are reconstructed using a particle-flow (PF) technique [30,31], in which signals from all CMS sub-detectors are combined to identify and reconstruct the individual particle candidates produced in the pp collision. The reconstructed particles include muons, electrons, photons, charged hadrons, and neutral hadrons. Charged particles are required to originate from the primary collision vertex, defined as the vertex with the highest sum of transverse momenta of all reconstructed tracks associated to it. Therefore, charged hadron candidates from pileup events, i.e. originating from a vertex other than the one of the hard interaction, are removed before jet clustering on an event-by-event basis. Subsequently, the remaining neutral-hadron pileup component is subtracted at the level of jet energy correction [32].

Electron candidates are reconstructed from a combination of their track and energy deposition in the ECAL [33]. In the dilepton channel, they are required to have a transverse momentum $p_{\mathrm{T}} > 20\,\mathrm{GeV}$, while in the $\ell$+jets channel they are required to have $p_{\mathrm{T}} > 30\,\mathrm{GeV}$. In both cases they are required to be reconstructed within $|\eta| < 2.4$, and electrons from identified photon conversions are rejected. As an additional quality criterion, a relative isolation variable $I_{\mathrm{rel}}$ is computed. This is defined as the sum of the $p_{\mathrm{T}}$ of all neutral and charged reconstructed PF candidates inside a cone around the lepton (excluding the lepton itself) in the $\eta$-$\phi$ plane with radius $\Delta R \equiv \sqrt{(\Delta\eta)^2 + (\Delta\phi)^2} < 0.3$, divided by the $p_{\mathrm{T}}$ of the lepton. In the dilepton (e+jets) channel, electrons are selected as isolated if $I_{\mathrm{rel}} < 0.12$ (0.10).

Muon candidates are reconstructed from tracks that can be matched between the silicon tracker and the muon system [34]. They are required to have a transverse momentum $p_{\mathrm{T}} > 20\,\mathrm{GeV}$ within the pseudorapidity interval $|\eta| < 2.4$ in the dilepton channel, and to have $p_{\mathrm{T}} > 30\,\mathrm{GeV}$ and $|\eta| < 2.1$ in the $\ell$+jets channel. Isolated muon candidates are selected by demanding a relative isolation of $I_{\mathrm{rel}} < 0.20$ (0.125) in the dilepton ($\mu$+jets) channel.

Jets are reconstructed by clustering the particle-flow candidates [35] using the anti-$k_{\mathrm{T}}$ algorithm with a distance parameter of 0.5 [36,37]. An offset correction is applied to take into account the extra energy clustered in jets due to pileup, using the FastJet algorithm [38] based on average pileup energy density in the event. The raw jet energies are corrected to establish a relative uniform response of the calorimeter in $\eta$ and a calibrated absolute response in $p_{\mathrm{T}}$. Jet energy corrections are derived from the simulation, and are confirmed with in situ measurements with the energy balance of dijet and photon+jet events [35]. Jets are selected within $|\eta| < 2.4$ and with $p_{\mathrm{T}} > 30$ (35) GeV in the dilepton ($\ell$+jets) channel.

Jets originating from b quarks or antiquarks are identified with the Combined Secondary Vertex algorithm [39], which provides a b-tagging discriminant by combining secondary vertices and track-based lifetime information. The chosen working point used in the dilepton channel corresponds to an efficiency for tagging a b jet of about 80–85 %, while the probability to misidentify light-flavour or gluon jets as b jets (mistag rate) is around 10 %. In the $\ell$+jets channel, a tighter requirement is applied, corresponding to a b-tagging efficiency of about 65–70 % with a mistag rate of 1 %. The probability to misidentify a c jet as b jet is about 40 % and 20 % for the working points used in the dilepton and $\ell$+jets channels respectively [39].

The missing transverse energy ($E_{\mathrm{T}}^{\mathrm{miss}}$) is defined as the magnitude of the sum of the momenta of all reconstructed PF candidates in the plane transverse to the beams.

### 4.2 Event selection

Dilepton events are collected using combinations of triggers which require two leptons fulfilling $p_{\mathrm{T}}$ and isolation criteria. During reconstruction, events are selected if they contain at least two isolated leptons (electrons or muons) of opposite charge and at least two jets, of which at least one is identified as a b jet. Events with a lepton pair invariant mass smaller than 12 GeV are removed in order to suppress events from heavy-flavour resonance decays. In the ee and $\mu\mu$ channels, the dilepton invariant mass is required to be outside a Z-boson mass window of $91 \pm 15\,\mathrm{GeV}$ (*Z-boson veto*), and $E_{\mathrm{T}}^{\mathrm{miss}}$ is required to be larger than 30 GeV.

A kinematic reconstruction method [5] is used to determine the kinematic properties of the $\mathrm{t\bar{t}}$ pair and to identify the two b jets originating from the decay of the top quark and antiquark. In the kinematic reconstruction the following constraints are imposed: the $E_{\mathrm{T}}^{\mathrm{miss}}$ originated entirely from the two neutrinos; the reconstructed W-boson invariant mass of 80.4 GeV [40] and the equality of the reconstructed top quark and antiquark masses. The remaining ambiguities are resolved by prioritising those event solutions with two or one b-tagged jets over solutions using untagged jets. Finally, among the physical solutions, the solutions are ranked according to how the neutrino energies match with a simulated neutrino energy spectrum and the highest ranked one is chosen. The kinematic reconstruction yields no valid solution for about 11 % of the events. These are excluded

from further analysis. A possible bias due to rejected solutions has been studied and found to be negligible.

In the e+jets channel, events are triggered by an isolated electron with $p_{\mathrm{T}} > 25\,\mathrm{GeV}$ and at least three jets with $p_{\mathrm{T}} > 30\,\mathrm{GeV}$. Events in the $\mu$+jets channel are triggered by the presence of an isolated muon with $p_{\mathrm{T}} > 24\,\mathrm{GeV}$ fulfilling $\eta$ requirements. Only triggered events that have exactly one high-$p_{\mathrm{T}}$ isolated lepton are retained in the analysis. In the e+jets channel, events are rejected if any additional electron is found with $p_{\mathrm{T}} > 20\,\mathrm{GeV}$, $|\eta| < 2.5$, and relative isolation $I_{\mathrm{rel}} < 0.20$. In the $\mu$+jets channel, events are rejected if any electron candidate with $p_{\mathrm{T}} > 15\,\mathrm{GeV}$, $|\eta| < 2.5$ and $I_{\mathrm{rel}} < 0.20$ is reconstructed. In both $\ell$+jets channels events with additional muons with $p_{\mathrm{T}} > 10\,\mathrm{GeV}$, $|\eta| < 2.5$, and relative isolation $I_{\mathrm{rel}} < 0.20$ are rejected. The presence of at least three reconstructed jets is required. At least two of them are required to be b-tagged.

Only $\mathrm{t\bar{t}}$ events from the decay channel under study are considered as signal. All other $\mathrm{t\bar{t}}$ events are considered as background, including those containing leptons from $\tau$ decays, which are the dominant contribution to this background.

### 4.3 Background estimation

After the full event selection is applied, the dominant background in the $\mathrm{e}\mu$ channel comes from other $\mathrm{t\bar{t}}$ decay modes, estimated using simulation. In the ee and $\mu\mu$ channels, it arises from $\mathrm{Z}/\gamma^*$+jets production. The normalisation of this background contribution is derived from data using the events rejected by the Z-boson veto, scaled by the ratio of events failing and passing this selection estimated in simulation ($R_{\mathrm{out/in}}$) [41]. The number of $\mathrm{Z}/\gamma^*$+jets $\rightarrow \mathrm{ee}/\mu\mu$ events near the Z-boson peak, $N^{\mathrm{in}}_{\mathrm{Z}/\gamma^*}$, is given by the number of all events failing the Z-boson veto, $N^{\mathrm{in}}$, after subtracting the contamination from non-$\mathrm{Z}/\gamma^*$+jets processes. This contribution is extracted from $\mathrm{e}\mu$ events passing the same selection, $N^{\mathrm{in}}_{\mathrm{e}\mu}$, and corrected for the differences between the electron and muon identification efficiencies using a correction factor $k$. The $\mathrm{Z}/\gamma^*$+jets contribution is thus given by

$$N^{\mathrm{out}} = R_{\mathrm{out/in}} N^{\mathrm{in}}_{\mathrm{Z}/\gamma^*} = R_{\mathrm{out/in}}(N^{\mathrm{in}} - 0.5 k N^{\mathrm{in}}_{\mathrm{e}\mu}) \quad (1)$$

The factor $k$ is estimated from $k^2 = N_{\mathrm{e}\mu}/N_{\mathrm{ee}}$ ($N_{\mathrm{e}\mu}/N_{\mu\mu}$) for the $\mathrm{Z}/\gamma^* \rightarrow \mathrm{e^+e^-}$ ($\mu^+\mu^-$)+jets contribution, respectively. Here $N_{\mathrm{ee}}$ ($N_{\mu\mu}$) is the number of ee ($\mu\mu$) events in the Z-boson region, without the requirement on $E^{\mathrm{miss}}_{\mathrm{T}}$. The remaining backgrounds, including single-top-quark, W+jets, diboson, and QCD multijet events are estimated from simulation.

In the $\ell$+jets channel, the main background contributions arise from W+jets and QCD multijet events, which are greatly suppressed by the b-tagging requirement. A procedure based on control samples in data is used to extract the QCD multijet background. The leptons in QCD multijet events are expected to be less isolated than leptons from other processes. Thus, inverting the selection on the lepton relative isolation provides a relatively pure sample of QCD multijet events in data. Events passing the standard event selection but with an $I_{\mathrm{rel}}$ between 0.3 and 1.0, and with at least one b-tagged jet are selected. The sample is divided in two: the sideband region (one b jet) and the signal region ($\geq$2 b jets). The shape of the QCD multijet background is taken from the signal region, and the normalisation is determined from the sideband region. In the sideband region, the $E^{\mathrm{miss}}_{\mathrm{T}}$ distribution of the QCD multijet model, other sources of background (determined from simulation), and the $\mathrm{t\bar{t}}$ signal are fitted to data. The resulting scaling of QCD multijet background is applied to the QCD multijet shape from the signal region.

Since the initial state of LHC collision is enriched in up quarks with respect to down quarks, more W bosons are produced with positive charge than negative charge. In leptonic W-boson decays, this translates into a lepton charge asymmetry $\mathcal{A}$. Therefore, a difference between the number of events with a positively charged lepton and those with a negatively charged lepton ($\Delta\pm$) is observed. In data, this quantity ($\Delta\pm^{\mathrm{data}}$) is proportional to the number of W+jets events when assuming that only the charge asymmetry from W-boson production is significant. The charge asymmetry has been measured by CMS [42] and found to be well described by the simulation, thus the simulated value can be used to extract the number of W+jets events from data: $N^{\mathrm{data}}_{\mathrm{W+jets}} = \Delta\pm^{\mathrm{data}}/\mathcal{A}$. The correction factor on the W+jets normalisation, calculated before any b-tagging requirement, is between 0.81 and 0.92 depending on the W decay channel and the jet selection. Subsequently, b-tagging is applied to obtain the number of W+jets events in the signal region.

In addition, a heavy-flavour correction must be applied on the W+jets sample to account for the differences observed between data and simulation [43]. Using the matching between selected jets and generated partons, simulated events are classified as containing at least one b jet (W+bX), at least one c jet and no b jets (W+cX), or containing neither b jets nor c jets (W+light quarks). The rate of W+bX events is multiplied by $2 \pm 1$ and the rate of W+cX events is multiplied by $1^{+1.0}_{-0.5}$. No correction is applied to W+light-jets events. These correction factors are calculated in [43] in a phase space which is close to the one used in the analysis. The uncertainties in the correction factors are taken into account as systematic uncertainties. The total number of W+jets events is modified to conserve this number when applying the heavy-flavour corrections. The remaining backgrounds, originating from single-top-quark, diboson, and $\mathrm{Z}/\gamma^*$+jets processes, are small and their contributions are estimated using simulation.

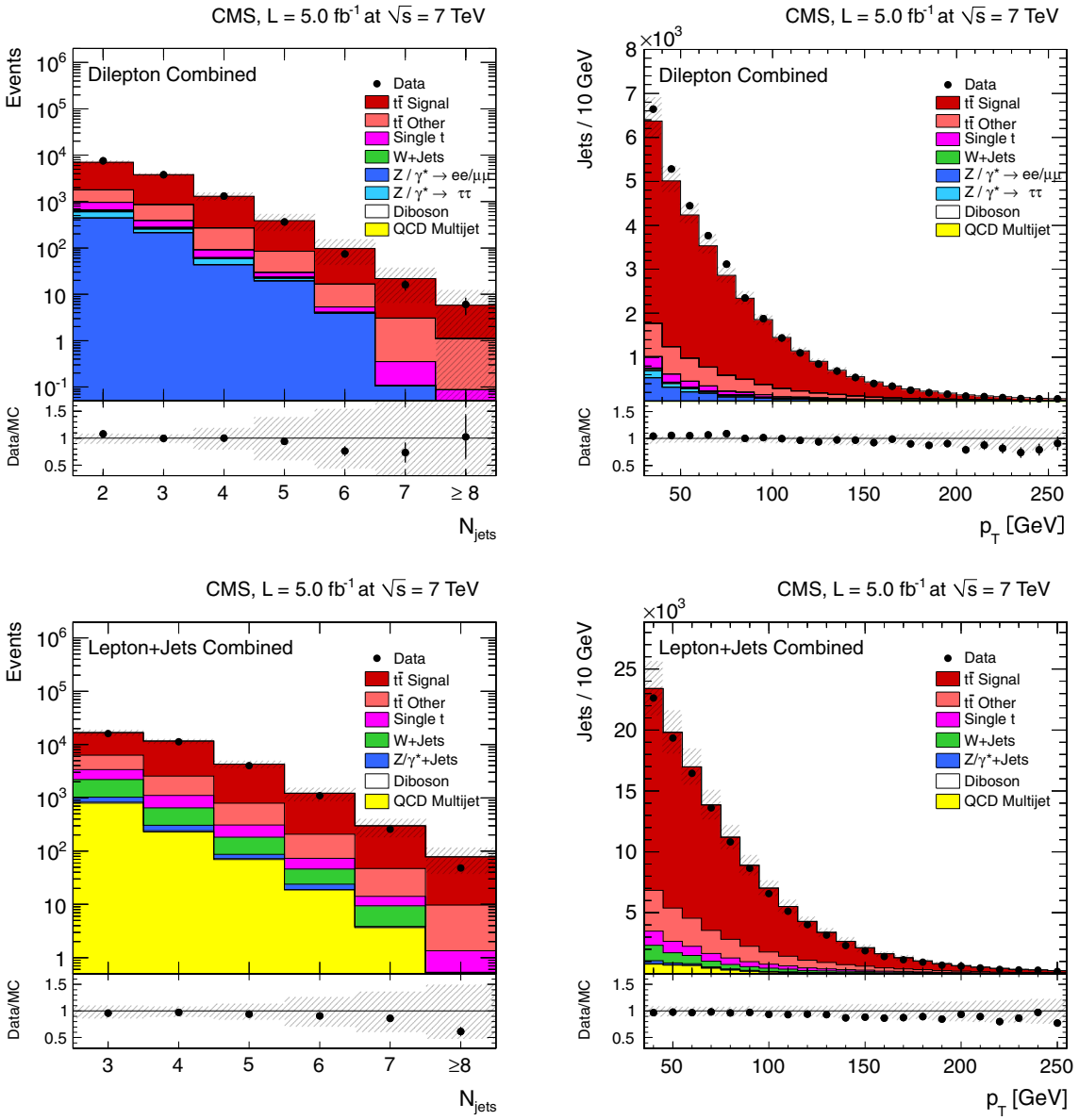


**Fig. 1** Number of reconstructed jets (*left*) and jet $p_{\mathrm{T}}$ spectrum (*right*) after event selection in the dilepton channel for jets with $p_{\mathrm{T}} > 30$ GeV (*top*), and in the $\ell$+jets channel for jets with $p_{\mathrm{T}} > 35$ GeV (*bottom*). The *hatched band* represents the combined effect of all sources of systematic uncertainty

The multiplicity and the $p_{\mathrm{T}}$ distributions of the selected reconstructed jets are shown for the dilepton and $\ell$+jets channels in Fig. 1. Good agreement for the jet multiplicity is observed between data and simulation for up to 5 (6) jets in the dilepton ($\ell$+jets) channels. For higher jet multiplicities, the simulation predicts slightly more events than observed in data. The modelling of the jet $p_{\mathrm{T}}$ spectrum in data is shifted towards smaller values, covered by the systematic uncertainties. The uncertainty from all systematic sources, which are described in Sect. 5, is determined by estimating their effect on both the normalisation and the shape. The size of these global uncertainties does not reflect those in the final measurements, since they are normalised and, therefore, only affected by shape uncertainties.

## 5 Systematic uncertainties

Systematic uncertainties in the measurement arise from detector effects, background modelling, and theoretical assumptions. Each systematic uncertainty is investigated separately and estimated for each bin of the measurement by varying the corresponding efficiency, resolution, or scale within its uncertainty. For each variation, the measured nor-

malised differential cross section is recalculated, and the difference between the varied result and the nominal result in each bin is taken as systematic uncertainty. The overall uncertainty in the measurement is obtained by adding all contributions in quadrature. The sources of systematic uncertainty, described below, are assumed to be uncorrelated.

- **Jet energy** The impact of the jet energy scale (JES) [35] is determined by varying the $p_{\mathrm{T}}$ of all jets by the JES uncertainty, which is typically below 3 %. The uncertainty due to the jet energy resolution (JER) [44] is estimated by varying the nominal value by $\pm 1\sigma$.
- $\mathrm{t\bar{t}}$ **model uncertainties** Uncertainties originating from theoretical assumptions on the renormalisation and factorisation scales, the jet-parton matching threshold, the hadronisation model, and the colour reconnection modelling [45], are determined by repeating the analysis, replacing the reference MadGraph signal simulation by other simulation samples. In particular, the impact of the former sources is assessed with MadGraph samples with the renormalisation and factorisation scales simultaneously varied from the nominal $Q^2$ values to $4Q^2$ and $Q^2/4$ and with jet-parton matching threshold varied to 40 and 10 GeV. The uncertainties from ambiguities in modeling colour reconnection effects are estimated by comparing simulations of an underlying event tune including colour reconnection to a tune without it (the Perugia 2011 and Perugia 2011 noCR tunes described in [46]). The hadronisation model uncertainty is estimated by comparing samples simulated with powheg and mc@nlo, using pythia and herwig, respectively, for hadronisation. The uncertainty arising from the PDFs is assessed by reweighting the $\mathrm{t\bar{t}}$ signal sample according to the 44 CTEQ66 error PDF sets, at 90 % confidence level. The effects of these variations are added in quadrature.
- **Background** The uncertainty due to the normalisation of the backgrounds that are taken from simulation is determined by varying the cross section by $\pm 30$ % [47,48]. This takes into account the uncertainty in the predicted cross section and all other sources of systematic uncertainty.
  In the dilepton channels, the contribution from $\mathrm{Z}/\gamma^*$+jets processes as determined from data is varied in normalisation by $\pm 30$ % [41].
  In the $\ell$+jets channels, the uncertainty in the W+jets background arises from the contamination of other processes with a lepton charge asymmetry when extracting the rate from data, and from the uncertainty in the heavy-flavour correction factors. The rate uncertainty is estimated to range from 10 to 20 %, depending on the channel. The model uncertainty is estimated using samples with varied renormalisation and factorisation scales and jet-parton matching threshold.
  The QCD multijet background modelling uncertainty arises from the choice of the relative isolation requirement on the anti-isolated lepton used for the extraction of the background from data, the influence of the contamination from other processes on the shape, and the extrapolation from the sideband to the signal region. The total uncertainty is about 15 % to more than 100 %, depending on the channel.
- **Other systematic uncertainties** The uncertainty associated with the pileup model is determined by varying the minimum bias cross section within its uncertainty of $\pm 8$ %. Other uncertainties taken into account originate from lepton trigger, isolation, and identification efficiencies; b-jet tagging efficiency and misidentification probability; integrated luminosity [49]; and the kinematic reconstruction algorithm used in the dilepton channels.

In the dilepton channels, the total systematic uncertainty is about 3 % at low jet multiplicities, and increases to about 20 % in the bins with at least five jets. In the $\ell$+jets channels, the total systematic uncertainty is about 6 % at the lowest jet multiplicity, and increases to 34 % for events with at least 8 jets.

The dominant systematic uncertainties for both dilepton and $\ell$+jets channels arise from the JES (with typical values from 2 to 20 %, depending on the jet multiplicity bin and cross section measurement) and the signal model including hadronisation, renormalisation and factorisation scales and jet-parton matching threshold (from 3 to 30 %). The typical systematic uncertainty due to JER ranges from 0.2 to 3 %, b-tagging from 0.3 to 2 %, pileup from 0.1 to 1.4 %, and background normalisation from 1.6 to 3.8 %. The uncertainty from other sources is below 0.5 %. The remaining uncertainties on the model arise from PDF and colour reconnection, varying from 0.1 to 1.5 % and from 1 to 5.8 %, respectively. In all channels, the systematic uncertainty for larger jet multiplicities is dominated by the statistical uncertainty of the simulated samples that are used for the evaluation of modelling uncertainties.

## 6 Normalised differential cross section as a function of jet multiplicity

The differential $\mathrm{t\bar{t}}$ production cross section as a function of the jet multiplicity is measured from the number of signal events after background subtraction and correction for the detector efficiencies and acceptances. The estimated number of background events arising from processes other that $\mathrm{t\bar{t}}$ production ($N_{\mathrm{non\ t\bar{t}\ BG}}$) is directly subtracted from the number of events in data ($N$). The contribution from other $\mathrm{t\bar{t}}$ decay modes is

**Table 1** Normalised differential $t\bar{t}$ production cross section as a function of the jet multiplicity for jets with $p_T > 30$ GeV in the dilepton channel. The statistical, systematic, and total uncertainties are also shown. The main experimental and model systematic uncertainties are displayed: JES and the combination of renormalisation and factorisation scales, jet-parton matching threshold, and hadronisation (in the table "$Q^2$/Match./Had.")

| $N_{jets}$ | $1/\sigma\, d\sigma/dN_{jets}$ | Stat. (%) | Exp. Syst. (%) | | Model Syst. (%) | | Total (%) |
|---|---|---|---|---|---|---|---|
| | | | JES | Other | $Q^2$/Match./Had. | Other | |
| 2 | 0.600 | 1.2 | 1.4 | 0.6 | 0.5 | 1.6 | 2.5 |
| 3 | 0.273 | 3.3 | 2.3 | 2.8 | 5.4 | 1.6 | 7.2 |
| 4 | 0.096 | 5.1 | 6.3 | 3.4 | 2.8 | 1.6 | 9.3 |
| 5 | 0.025 | 10.1 | 7.9 | 3.0 | 17.4 | 1.9 | 24.0 |
| ≥6 | 0.0013 | 23.8 | 14.2 | 2.8 | 24.3 | 2.1 | 37.1 |

**Table 2** Normalised differential $t\bar{t}$ production cross section as a function of the jet multiplicity for jets with $p_T > 60$ GeV in the dilepton channel. The statistical, systematic, and total uncertainties are also shown. The main experimental and model systematic uncertainties are displayed: JES and the combination of renormalisation and factorisation scales, jet-parton matching threshold, and hadronisation (in the table "$Q^2$/Match./Had.")

| $N_{jets}$ | $1/\sigma\, d\sigma/dN_{jets}$ | Stat. (%) | Exp. Syst. (%) | | Model Syst. (%) | | Total (%) |
|---|---|---|---|---|---|---|---|
| | | | JES | Other | $Q^2$/Match./Had. | Other | |
| 0 | 0.158 | 3.4 | 7.0 | 5.7 | 2.7 | 1.6 | 10.1 |
| 1 | 0.397 | 4.0 | 4.9 | 2.0 | 3.3 | 1.9 | 7.6 |
| 2 | 0.350 | 2.6 | 3.2 | 3.3 | 3.5 | 1.7 | 6.6 |
| 3 | 0.079 | 5.2 | 3.4 | 3.0 | 5.8 | 1.6 | 9.2 |
| 4 | 0.0127 | 13.9 | 5.4 | 3.5 | 15.8 | 1.7 | 22.1 |
| 5 | 0.0020 | 30.9 | 4.8 | 3.6 | 15.5 | 1.6 | 35.1 |
| ≥6 | 0.00012 | 57.1 | 4.7 | 16.7 | 38.7 | 2.9 | 69.4 |

taken into account by correcting $N - N_{\text{non } t\bar{t}\text{ BG}}$ with the signal fraction, defined as the ratio of the number of selected $t\bar{t}$ signal events to the total number of selected $t\bar{t}$ events. This avoids the dependence on the inclusive $t\bar{t}$ cross section used for normalisation. The normalised differential cross section is derived by scaling to the total integrated luminosity and by dividing the corrected number of events by the cross section measured in situ for the same phase space. Because of the normalisation, those systematic uncertainties that are correlated across all bins of the measurement, and therefore only affect the normalisation, cancel out. In order to avoid additional uncertainties due to the extrapolation of the measurement outside of the phase space region probed experimentally, the differential cross section is determined in a visible phase space defined at the particle level by the kinematic and geometrical acceptance of the final-state leptons and jets.

The visible phase space at particle level is defined as follows. The charged leptons from the $t\bar{t}$ decays are selected with $|\eta| < 2.4$ in dilepton events and $|\eta| < 2.5\,(2.1)$ in e+jets ($\mu$+jets) final states, $p_T > 20\,(30)$ GeV in the dilepton ($\ell$+jets) channels. A jet is defined at the particle level in a similar way as described in Sect. 4 for the reconstructed jets, by applying the anti-$k_T$ clustering algorithm to all stable particles (including neutrinos not coming from the hard interaction). Particle-level jets are rejected if the selected leptons are within a cone of $\Delta R = 0.4$ with respect to the jet, to avoid counting leptons misidentified as jets. A jet is defined as a b jet if it contains the decay products of a b hadron. The two b jets from the $t\bar{t}$ decay have to fulfill the kinematic requirements $|\eta| < 2.4$ and $p_T > 30\,(35)$ GeV in the dilepton ($\ell$+jets) events. In the $\ell$+jets channels, a third jet with the same properties is also required.

Effects from trigger and detector efficiencies and resolutions, leading to migrations of events across bin boundaries and statistical correlations among neighbouring bins, are corrected by using a regularised unfolding method [5,50,51]. A response matrix that accounts for migrations and efficiencies is calculated from simulated $t\bar{t}$ events using the reference MadGraph sample. The event migration in each bin is controlled by the purity (number of events reconstructed and generated in one bin divided by the total number of reconstructed events in that bin) and the stability (number of events reconstructed and generated in one bin divided by the total number of generated events in that bin). In these measurements, the purity and stability in the bins is typically 60 % or higher. The generalised inverse of the response matrix is used to obtain

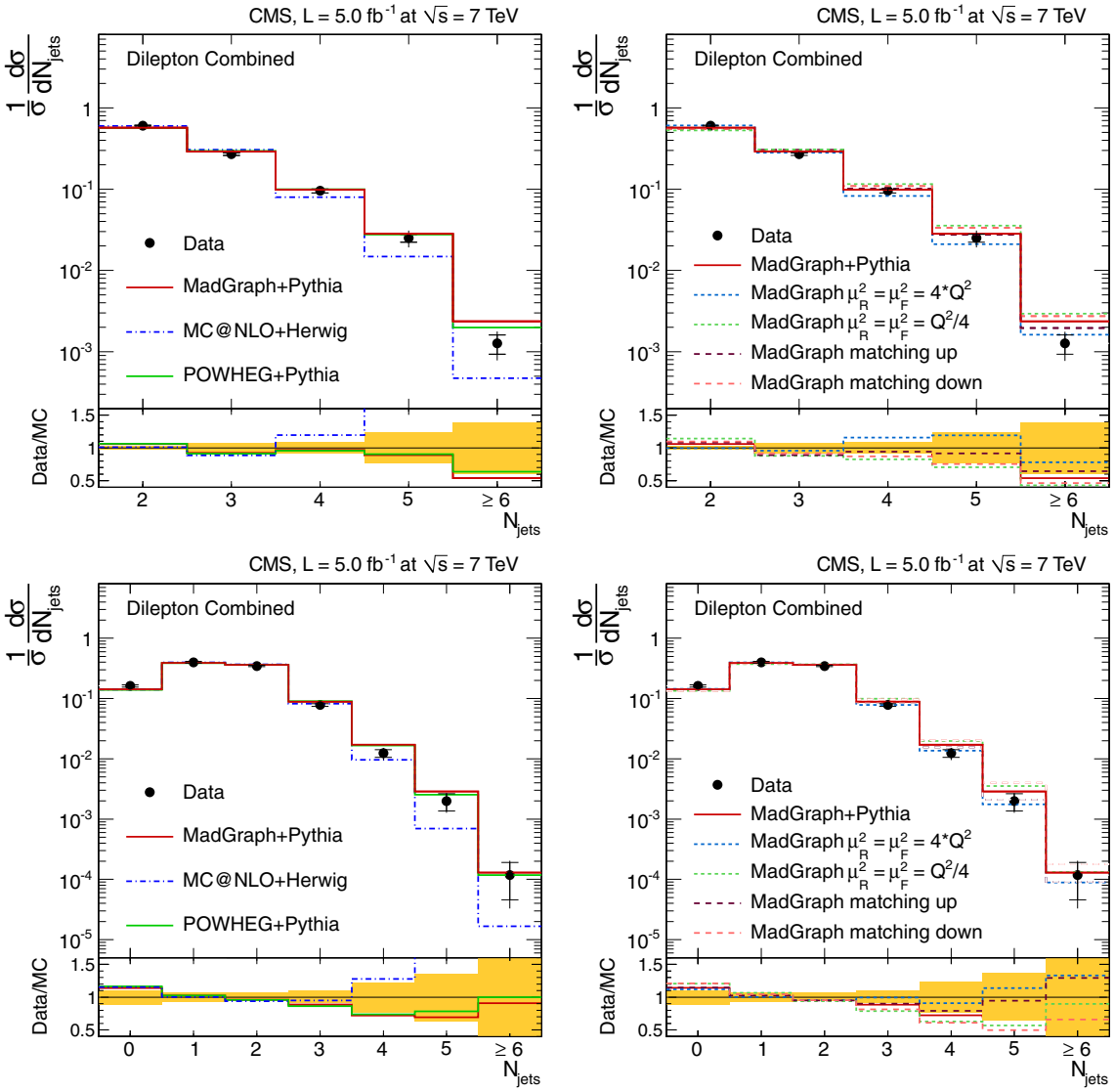


**Fig. 2** Normalised differential $t\bar{t}$ production cross section as a function of the jet multiplicity for jets with $p_T$ >30 GeV (*top*) and $p_T$ > 60 GeV (*bottom*) in the dilepton channel. The measurements are compared to predictions from MADGRAPH+PYTHIA, POWHEG+PYTHIA, and MC@NLO+HERWIG (*left*), as well as from MADGRAPH with varied renormalisation and factorisation scales, and jet-parton matching threshold (*right*). The *inner* (*outer*) *error bars* indicate the statistical (combined statistical and systematic) uncertainty. The *shaded band* corresponds to the combined statistical and systematic uncertainty

the unfolded distribution from the measured distribution by applying a $\chi^2$ technique. To avoid non-physical fluctuations, a smoothing prescription (regularisation) is applied [5,52]. The unfolded data are subsequently corrected to take into account the acceptance in the particle level phase space.

The measured normalised differential cross sections are consistent among the different dilepton and $\ell$+jets channels. The final results in the dilepton and $\ell$+jets channels are obtained from the weighted average of the individual measurements, using the statistical uncertainty as the weight. The result from the combination of e+jets and $\mu$+jets channels is defined for the pseudorapidity range $|\eta| < 2.1$, i.e. according to the selection criterion of the $\mu$+jets channel. The difference of this result to that for the pseudorapidity range $|\eta| < 2.5$ has been estimated to be less than 0.4 % in any of the bins of the jet multiplicity distribution. In the combination, the differences in the $|\eta|$-range between $\mu$+jets and e+jets channels are therefore neglected.

The normalised differential $t\bar{t}$ production cross section, $1/\sigma\, d\sigma/dN_{jets}$, as a function of the jet multiplicity, $N_{jets}$, is shown in Tables 1 and 2, and Fig. 2 for the dilepton channel and jets with $p_T > 30$ (60) GeV. For the $\ell$+jets channel it is shown in Table 3 and Fig. 3 for jets with $p_T > 35$ GeV. In the tables, the experimental uncertainties are divided between

**Table 3** Normalised differential $t\bar{t}$ production cross section as a function of the jet multiplicity for jets with $p_T > 35$ GeV in the $\ell$+jets channel. The statistical, systematic, and total uncertainties are also shown. The main experimental and model systematic uncertainties are displayed: JES and the combination of renormalisation and factorisation scales, jet-parton matching threshold, and hadronisation (in the table "$Q^2$/Match./Had.")

| $N_{jets}$ | $1/\sigma\ d\sigma/dN_{jets}$ | Stat. (%) | Exp. Syst. (%) | | Model Syst. (%) | | Total (%) |
|---|---|---|---|---|---|---|---|
| | | | JES | Other | $Q^2$/Match./Had. | Other | |
| 3 | 0.453 | 0.9 | 3.8 | 2.2 | 3.8 | 1.3 | 6.1 |
| 4 | 0.372 | 1.2 | 1.8 | 1.8 | 3.2 | 1.4 | 4.5 |
| 5 | 0.130 | 2.7 | 5.6 | 2.0 | 7.5 | 1.8 | 10.2 |
| 6 | 0.0353 | 5.3 | 6.7 | 2.4 | 14.2 | 2.5 | 17.0 |
| 7 | 0.00841 | 10.5 | 10.7 | 3.3 | 19.1 | 4.3 | 24.9 |
| ≥8 | 0.00130 | 26.4 | 17.7 | 5.1 | 28.6 | 3.4 | 43.2 |

the dominant (JES) and other (JER, b-tagging, pileup, lepton identification, isolation, and trigger efficiencies, background contribution and integrated luminosity) contributions. The model uncertainties are also divided between the dominant (renormalisation and factorisation scales, jet-parton matching threshold, and hadronisation) and other (PDF and colour reconnection) contributions. The measurements are compared to the predictions from MadGraph and powheg, both interfaced with pythia, and from mc@nlo interfaced with herwig.

The predictions from MadGraph+pythia and powheg +pythia are found to provide a reasonable description of the data. In contrast, mc@nlo+herwig generates fewer events in bins with large jet multiplicities. The effect of the variation of the renormalisation and factorisation scales and jet-parton matching threshold in MadGraph+pythia is compared with the reference MadGraph+pythia simulation. The choice of lower values for both these parameters seems to provide a worse description of the data for higher jet multiplicities.

## 7 Normalised differential cross section as a function of the additional jet multiplicity

The normalised differential $t\bar{t}$ production cross section is also determined as a function of the number of additional jets accompanying the $t\bar{t}$ decays in the $\ell$+jets channel. This measurement provides added value to the one presented in Sect. 6 by distinguishing jets from the $t\bar{t}$ decay products and jets coming from additional QCD radiation. This is particularly interesting in final states with many jets.

For this measurement, the event selection follows the prescription discussed in Sect. 4, and requires at least four jets (in order to perform a full event reconstruction later) with $p_T > 30$ GeV and $|\eta| < 2.4$. The $p_T$ requirement is lowered to gain more data and reduce the statistical uncertainty. The particle-level jets, defined as described in Sect. 6 but with $p_T > 30$ GeV, are counted as additional jets if their distance to the $t\bar{t}$ decay products is $\Delta R > 0.5$. We consider the following objects as $t\bar{t}$ decay products: two b quarks, two light quarks from the hadronically decaying $W$ boson, and the lepton from the leptonically decaying $W$ boson; the neutrino is not included. The simulated $t\bar{t}$ events are classified into three categories according to the number of additional jets (0, 1, and ≥2) selected according to this definition. Figure 4 illustrates the contributions of $t\bar{t}$ events with 0, 1, and ≥2 additional jets to the number of reconstructed jets in the simulation.

A full event reconstruction of the $t\bar{t}$ system is performed in order to create a variable sensitive to additional jets, taking into account all possible jet permutations. The most likely permutation is determined using a $\chi^2$ minimisation, where the $\chi^2$ is given by:

$$\chi^2 = \left(\frac{m_{W^{had}}^{rec} - m_{W^{had}}^{true}}{\sigma_{W^{had}}}\right)^2 + \left(\frac{m_{t^{had}}^{rec} - m_{t^{had}}^{true}}{\sigma_{t^{had}}}\right)^2 + \left(\frac{m_{t^{lep}}^{rec} - m_{t^{lep}}^{true}}{\sigma_{t^{lep}}}\right)^2,$$

where $m_{t^{had}}^{rec}$ and $m_{t^{lep}}^{rec}$ are the reconstructed invariant masses of the hadronically and the leptonically decaying top quark, respectively, and $m_{W^{had}}$ is the reconstructed invariant mass of the W boson from the hadronic top-quark decay. The parameters $m^{true}$ and $\sigma_{t^{had}}$, $\sigma_{t^{lep}}$, and $\sigma_{W^{had}}$ are the mean value and standard deviations of the reconstructed mass distributions in the $t\bar{t}$ simulation. In each event, all jet permutations in which only b-tagged jets are assigned to b quarks are considered. The permutation with the smallest $\chi^2$ value is chosen as the best hypothesis. For events containing the same number of reconstructed jets ($N_{jets}$) the variable $\sqrt{\chi^2}$ provides good discrimination between events classified as $t\bar{t}$ + 0, 1, and ≥2 additional jets. The discrimination power is due to the sensitivity of the event reconstruction to the relation between $N_{jets}$

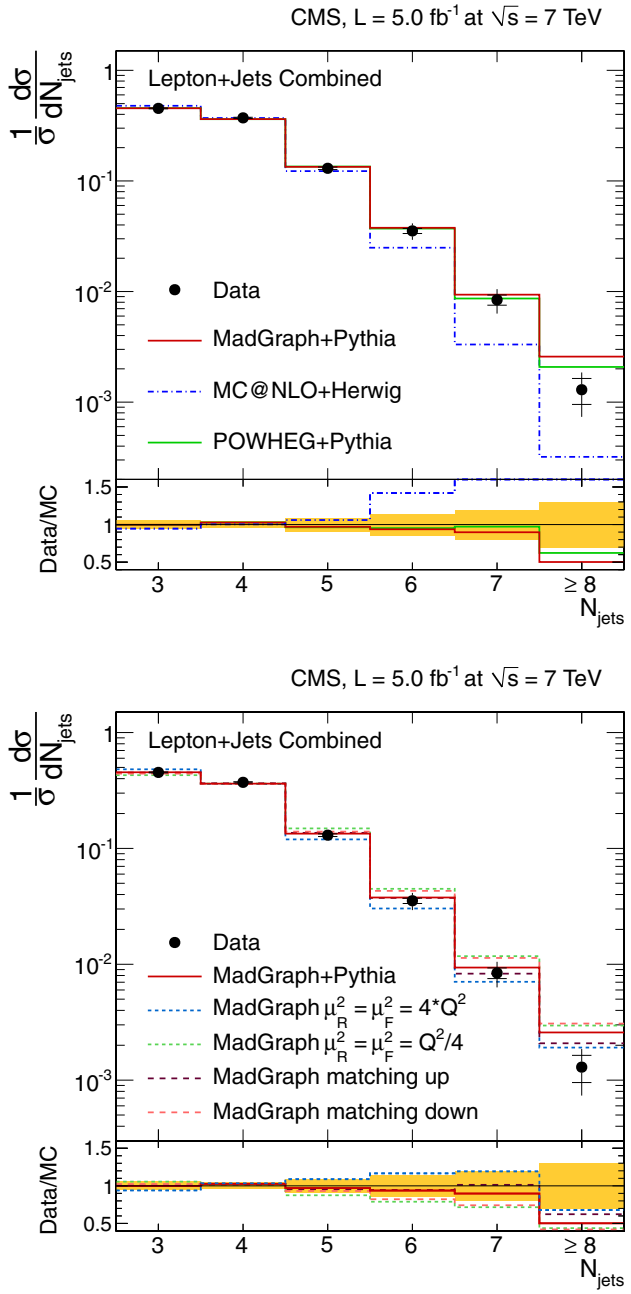


**Fig. 3** Normalised differential $t\bar{t}$ production cross section as a function of jet multiplicity for jets with $p_T > 35$ GeV in the $\ell$+jets channel. The measurement is compared to predictions from MADGRAPH+PYTHIA, POWHEG+PYTHIA, and MC@NLO+HERWIG (*top*), as well as from MADGRAPH with varied renormalisation and factorisation scales, and jet-parton matching threshold (*bottom*). The *inner* (*outer*) *error bars* indicate the statistical (combined statistical and systematic) uncertainty. The *shaded band* corresponds to the combined statistical and systematic uncertainty

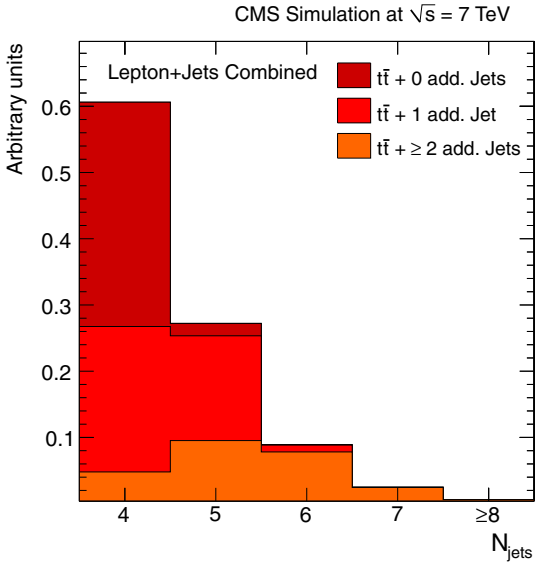


**Fig. 4** Jet multiplicity distribution in simulated $t\bar{t}$ events in the $\ell$+jets channel. The splitting into three categories, defined by the compatibility of the selected particle level jets with the $t\bar{t}$ decay partons is also shown (cf. Sect. 7)

and the number of additional jets $N_{\text{add. jets}}$. The best event reconstruction, thus providing a smaller $\sqrt{\chi^2}$, is achieved if the observation is close to $N_{\text{jets}} = 4 + N_{\text{add. jets}}$, where four is the expected number of jets from the $t\bar{t}$ decay partons. For instance, a $t\bar{t}$ + 1 additional jet event with $N_{\text{jets}} = 4$ is likely to get a large $\sqrt{\chi^2}$ value because one of the four jets from the $t\bar{t}$ decay partons is missing for a correct event reconstruction.

The measurement of the fractions of $t\bar{t}$ events with 0, 1, and $\geq$2 additional jets is performed using a binned maximum-likelihood fit of the $\sqrt{\chi^2}$ templates to data, simultaneously in both $\ell$+jets channels. The normalisations of the signal templates ($t\bar{t}$ + 0, 1, and $\geq$2 additional jets) are free parameters in the fit. For the normalisations of the background processes, Gaussian constraints corresponding to the uncertainties of the background predictions are applied. It has been verified that the use of log-normal constraints gives similar results. The result of the fit is shown in Fig. 5. The QCD multijet and W+jets templates are estimated using the data-based methods described in Sect. 4.

The normalisations for the three signal templates are applied to the predicted differential cross section in the visible phase space, calculated using the simulated $t\bar{t}$ sample from MADGRAPH+PYTHIA. This phase space is defined as in Sect. 6 with the requirement of four particle level jets with $p_T > 30$ GeV. This provides the differential cross section as a function of the number of additional jets, which is finally normalised to the total cross section measured in the same phase space. The results are shown in Fig. 6 and summarised in Table 4.

For each $t\bar{t}$ + additional jet template used in the maximum-likelihood fit, a full correlation is assumed between the rate of events that fulfill the particle-level selection and the rate of events that do not. Therefore, a single template is used for both parts.

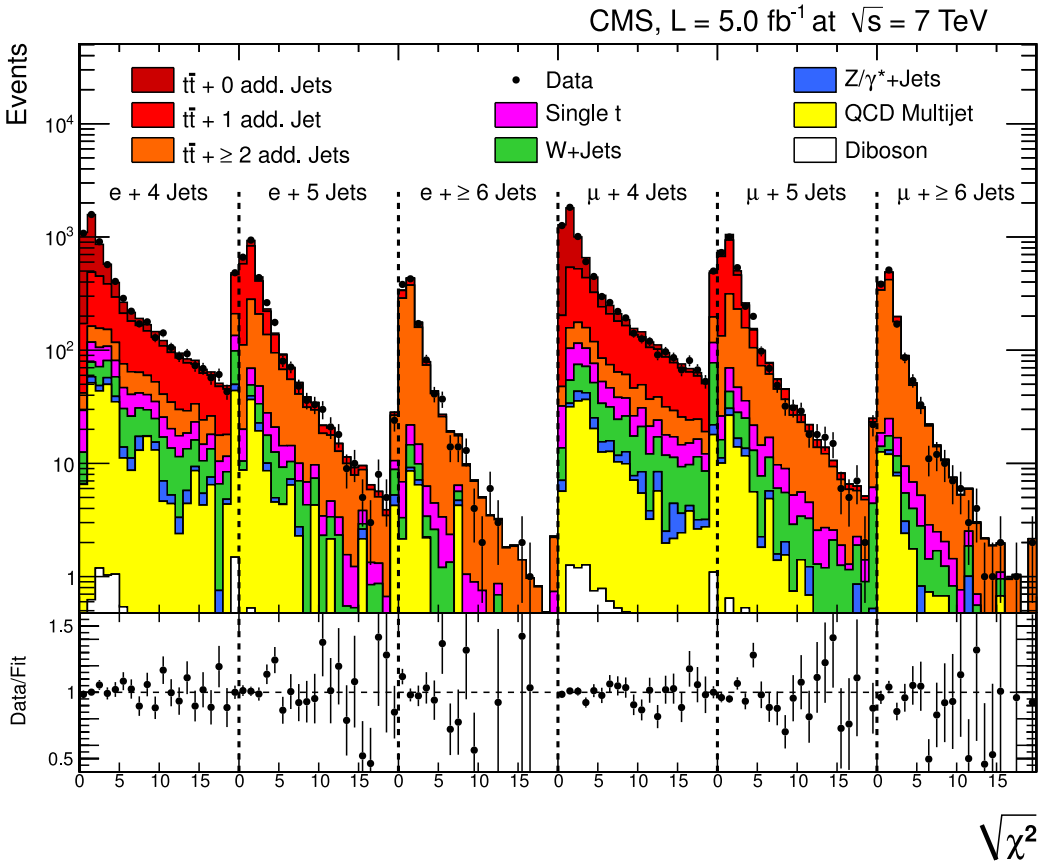


**Fig. 5** Result of the simultaneous template fit to the $\sqrt{\chi^2}$ distribution in the $\ell$+jets channel. All templates are scaled to the resulting fit parameters

Including an additional template made from events that are not inside the visible phase space leads to fit results that are compatible within the estimated uncertainties. To check the model dependency, the fit is repeated using simulated data from MC@NLO+HERWIG and POWHEG+PYTHIA instead of MADGRAPH+PYTHIA. The results are stable within the uncertainties.

The sources of systematic uncertainties are the same as those discussed in Sect. 5, except for the background normalisations, which are constrained in the fit. Their effect is propagated to the fit uncertainty, which is quoted as the statistical uncertainty. The impact of the systematic uncertainties on the extracted fractions of $\mathrm{t\bar{t}}$ + 0, 1, and $\geq$2 additional jets is evaluated using pseudo-experiments. The most important contributions to the systematic uncertainties originate from JES (up to 7 %) and modelling uncertainties: hadronisation (up to 6 %), jet-parton matching threshold (up to 5 %), and renormalisation and factorisation scales (up to 4 %).

The MC@NLO+HERWIG prediction produces fewer events with $\geq$2 additional jets than data, which are well described by MADGRAPH+PYTHIA and POWHEG+PYTHIA. The prediction from MADGRAPH+PYTHIA with lower renormalisation and factorisation scales provides a worse description of the data. These observations are in agreement with those presented in Sect. 6.

## 8 Additional jet gap fraction

An alternative way to investigate the jet activity arising from quark and gluon radiation produced in association with the $\mathrm{t\bar{t}}$ system is to determine the fraction of events that do not contain additional jets above a given threshold. This measurement is performed using events in the dilepton decay channel after fulfilling the event reconstruction and selection requirements discussed in Sect. 4. The additional jets are defined as those not assigned to the $\mathrm{t\bar{t}}$ system by the kinematic reconstruction described in Sect. 4.2.

A threshold observable, referred to as gap fraction [6], is defined as:

$$f(p_{\mathrm{T}}) = \frac{N(p_{\mathrm{T}})}{N_{\mathrm{total}}}, \tag{2}$$

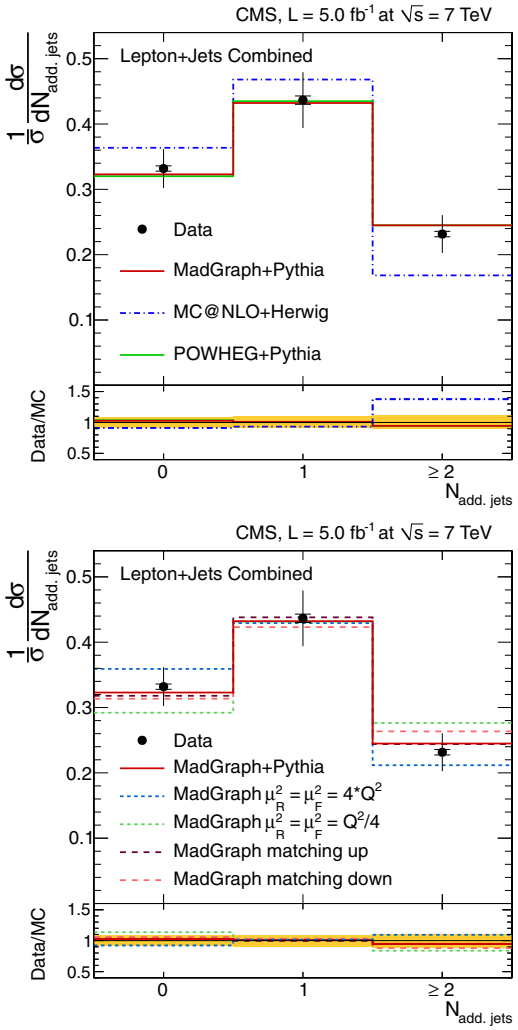


**Fig. 6** Normalised differential $t\bar{t}$ production cross section as a function of the number of additional jets in the $\ell$+jets channel. The measurement is compared to predictions from MADGRAPH+PYTHIA, POWHEG+PYTHIA, and MC@NLO+HERWIG (*top*), as well as from MADGRAPH with varied renormalisation and factorisation scales, and jet-parton matching threshold (*bottom*). The *inner* (*outer*) *error bars* indicate the statistical (combined statistical and systematic) uncertainty. The *shaded band* corresponds to the combined statistical and systematic uncertainty

where $N_{\text{total}}$ is the number of selected events and $N(p_{\text{T}})$ is the number of events that do not contain additional jets above a $p_{\text{T}}$ threshold in the whole pseudorapidity range used in the analysis ($|\eta| < 2.4$). The pseudorapidity and $p_{\text{T}}$ distributions of the first and second leading (in $p_{\text{T}}$) additional reconstructed jets are presented in Fig. 7. The distributions show good agreement between data and the simulation.

The veto can be extended beyond the additional leading jet criteria by defining the gap fraction as

$$f(H_{\text{T}}) = \frac{N(H_{\text{T}})}{N_{\text{total}}}, \tag{3}$$

where $N(H_{\text{T}})$ is the number of events in which $H_{\text{T}}$, the scalar sum of the $p_{\text{T}}$ of the additional jets (with $p_{\text{T}} > 30$ GeV), is less than a certain threshold.

For each value of $p_{\text{T}}$ and $H_{\text{T}}$ thresholds, the gap fraction is evaluated at particle level in the visible phase space defined in Sect. 6. The additional jets at particle level are defined as all jets within the kinematic acceptance not including the two highest-$p_{\text{T}}$ b jets containing the decay products of different b hadrons. They are required to fulfill the condition that they are not within a cone of $\Delta R = 0.4$ from any of the two isolated leptons, as described in Sect. 6.

Given the large purity of the selected events for any value of $p_{\text{T}}$ and $H_{\text{T}}$, a correction for detector effects is applied following a simpler approach than the unfolding method used in Sect. 6. Here, the ratio of the particle-level to the simulated gap fraction distributions, obtained with the $t\bar{t}$ sample from MADGRAPH, provides the correction which is applied to the data.

The measured gap-fraction distribution is compared to predictions from MADGRAPH+PYTHIA, POWHEG+PYTHIA, and MC@NLO+HERWIG, and to the predictions from the MADGRAPH samples with varied renormalisation and factorisation scales and jet-parton matching threshold. In Fig. 8 the gap fraction is measured as a function of the $p_{\text{T}}$ of the leading additional jet (left) and as a function of $H_{\text{T}}$ (right), with the thresholds (defined at the abscissa where the data point is shown) varied between 35 and 380 GeV.

**Table 4** Normalised differential $t\bar{t}$ production cross section as a function of the jet multiplicity for jets with $p_{\text{T}} > 30$ GeV in the dilepton channel. The statistical, systematic, and total uncertainties are also shown. The main experimental and model systematic uncertainties are displayed: JES and the combination of renormalisation and factorisation scales, jet-parton matching threshold, and hadronisation (in the table "$Q^2$/Match./Had.")

| $N_{\text{jets}}$ | $1/\sigma\, \mathrm{d}\sigma/\mathrm{d}N_{\text{add. jets}}$ | Stat. (%) | Exp. Syst. (%) | | Model Syst. (%) | | Total (%) |
|---|---|---|---|---|---|---|---|
| | | | JES | Other | $Q^2$/Match./Had. | Other | |
| $t\bar{t}$ + 0 add. Jets | 0.332 | 1.2 | 4.2 | 1.4 | 7.5 | 1.6 | 9.0 |
| $t\bar{t}$ + 1 add. Jet | 0.436 | 1.5 | 0.9 | 1.0 | 9.5 | 1.3 | 9.8 |
| $t\bar{t}$ + ≥2 add. Jets | 0.232 | 1.8 | 7.2 | 1.5 | 9.6 | 2.6 | 12.5 |

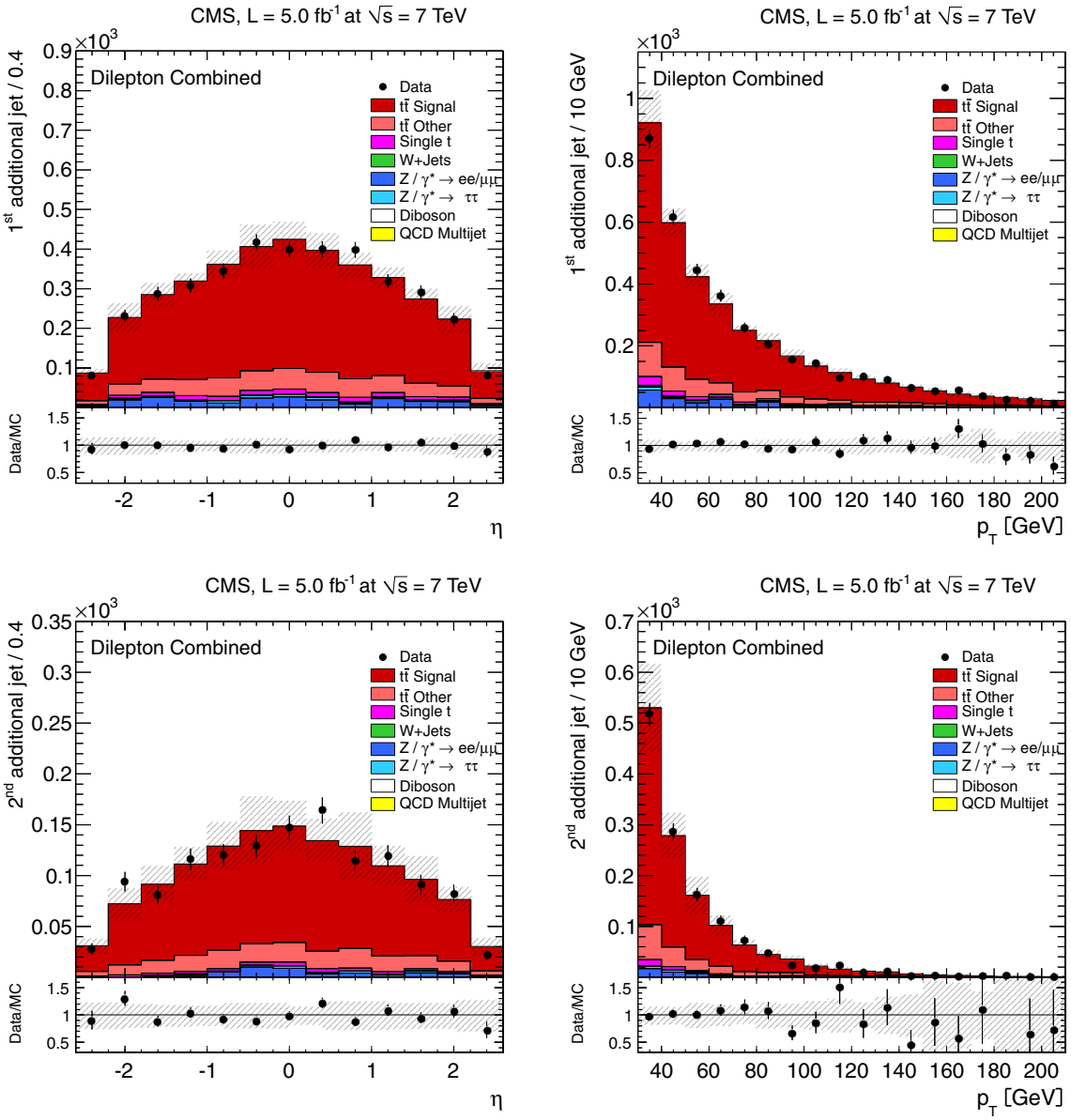


**Fig. 7** Distribution of the $\eta$ (*left*) and the $p_{\mathrm{T}}$ (*right*) of the first (*top*) and second (*bottom*) leading additional reconstructed jets compared to signal and background simulated samples. The *error bars* on the data points indicate the statistical uncertainty. The *hatched band* represents the combined effect of all sources of systematic uncertainty

The results are summarised in Tables 5 and 6, respectively. The measurements are consistent among the three dilepton channels. The gap fraction is lower as a function of $H_{\mathrm{T}}$ showing that the measurement is probing quark and gluon emission beyond the first emission. The gap fraction is better described by MC@NLO +HERWIG compared to MADGRAPH+PYTHIA and POWHEG+PYTHIA. This result is not incompatible with the observation described above, because the gap fraction requires the jets to have a certain $p_{\mathrm{T}}$ above the threshold, which does not imply necessarily large jet multiplicities. Decreasing the renormalisation and factorisation scales or matching threshold in the MADGRAPH sample worsens the agreement between data and simulation.

The total systematic uncertainty is about 3.5 % for values of the threshold ($p_{\mathrm{T}}$ or $H_{\mathrm{T}}$) below 40 GeV, and decreases to 0.2 % for values of the thresholds above 200 GeV. Dominant sources of systematic uncertainty arise from the uncertainty in the JES and the background contamination, corresponding to approximately 2 and 1 % systematic uncertainty, respectively, for the smallest $p_{\mathrm{T}}$ and $H_{\mathrm{T}}$ values. Other sources with smaller impact on the total uncertainty are the b-tagging efficiency, JER, pileup, and the procedure used to correct the data to particle level.

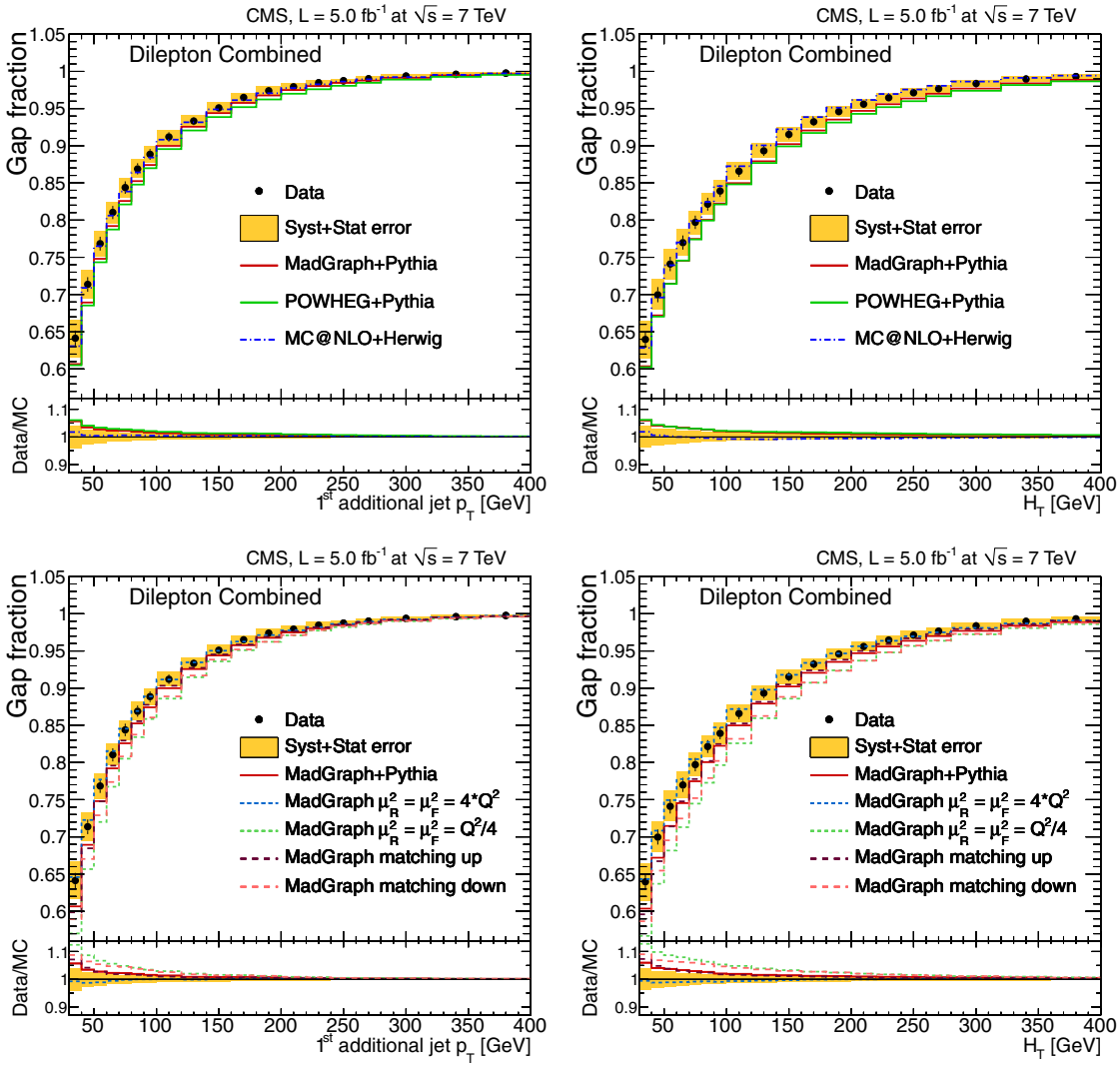


**Fig. 8** Measured gap fraction as a function of the additional jet $p_{\mathrm{T}}$ (*left*) and of $H_{\mathrm{T}} = \sum p_{\mathrm{T}}^{\text{add. jets}}$ (*right*) in the dilepton channels. Data are compared to predictions from MADGRAPH+PYTHIA, POWHEG+PYTHIA, and MC@NLO+HERWIG (*top*), as well as from MADGRAPH with varied renormalisation and factorisation scales, and jet-parton matching threshold (*bottom*). The *error bars* on the data points indicate the statistical uncertainty. The *shaded band* corresponds to the combined statistical and total systematic uncertainty (added in quadrature)

## 9 Summary

Measurements of the normalised differential $\mathrm{t\bar{t}}$ production cross section as a function of the number of jets in the dilepton (ee, $\mu\mu$, and e$\mu$) and $\ell$+jets (e+jets, $\mu$+jets) channels are presented. The measurements are performed using a data sample corresponding to an integrated luminosity of 5.0 fb$^{-1}$ collected in pp collisions at $\sqrt{s} = 7$ TeV with the CMS detector. The results are presented in the visible phase space and compared with predictions of perturbative quantum chromodynamics from MADGRAPH and POWHEG interfaced with PYTHIA, and MC@NLO interfaced with HERWIG, as well as MADGRAPH with varied renormalisation and factorisation scales, and jet-parton matching threshold. The normalised differential $\mathrm{t\bar{t}}$ production cross section is also measured as a function of the jets radiated in addition to the $\mathrm{t\bar{t}}$ decay products in the $\ell$+jets channel. The MADGRAPH+PYTHIA and POWHEG+PYTHIA predictions describe the data well up to high jet multiplicities, while MC@NLO+HERWIG predicts fewer events with large number of jets. The gap fraction is measured in dilepton events as a function of the $p_{\mathrm{T}}$ of the leading additional jet and the scalar sum of the $p_{\mathrm{T}}$ of the additional jets, and is also compared to different theoretical predictions. No significant deviations are observed between data and simulation. The MC@NLO+HERWIG model seems to more accurately describe the gap fraction for all values of the thresholds compared to MADGRAPH+PYTHIA and POWHEG+PYTHIA.

**Table 5** Measured gap fraction as a function of the additional jet $p_T$. The statistical, systematic, and total uncertainties are also shown

| $p_T$ Threshold (GeV) | Result | Stat. (%) | Syst. (%) | Total (%) |
|---|---|---|---|---|
| 35 | 0.64 | 1.7 | 3.5 | 3.9 |
| 45 | 0.70 | 1.4 | 2.6 | 3.0 |
| 55 | 0.74 | 1.3 | 2.4 | 2.7 |
| 65 | 0.77 | 1.2 | 2.0 | 2.3 |
| 75 | 0.80 | 1.1 | 1.6 | 2.0 |
| 85 | 0.82 | 1.0 | 1.4 | 1.8 |
| 95 | 0.84 | 1.0 | 1.4 | 1.7 |
| 110 | 0.87 | 0.9 | 1.1 | 1.4 |
| 130 | 0.89 | 0.8 | 0.8 | 1.1 |
| 150 | 0.92 | 0.7 | 0.8 | 1.1 |
| 170 | 0.93 | 0.6 | 0.6 | 0.8 |
| 190 | 0.95 | 0.6 | 0.5 | 0.7 |
| 210 | 0.96 | 0.5 | 0.5 | 0.7 |
| 230 | 0.96 | 0.4 | 0.5 | 0.6 |
| 250 | 0.97 | 0.4 | 0.4 | 0.6 |
| 270 | 0.98 | 0.4 | 0.4 | 0.5 |
| 300 | 0.98 | 0.3 | 0.3 | 0.5 |
| 340 | 0.99 | 0.3 | 0.3 | 0.4 |
| 380 | 0.99 | 0.2 | 0.2 | 0.3 |

**Table 6** Measured gap fraction as a function of $H_T = \sum p_T^{\text{add. jets}}$. The statistical, systematic, and total uncertainties are also shown

| $H_T$ Threshold (GeV) | Result | Stat. (%) | Syst. (%) | Total (%) |
|---|---|---|---|---|
| 35 | 0.64 | 1.6 | 3.6 | 3.9 |
| 45 | 0.71 | 1.4 | 2.3 | 2.6 |
| 55 | 0.77 | 1.2 | 1.9 | 2.3 |
| 65 | 0.81 | 1.1 | 1.4 | 1.8 |
| 75 | 0.84 | 1.0 | 1.2 | 1.5 |
| 85 | 0.87 | 0.9 | 1.1 | 1.4 |
| 95 | 0.89 | 0.8 | 1.0 | 1.3 |
| 110 | 0.91 | 0.7 | 0.8 | 1.1 |
| 130 | 0.93 | 0.6 | 0.6 | 0.8 |
| 150 | 0.95 | 0.5 | 0.6 | 0.8 |
| 170 | 0.96 | 0.4 | 0.5 | 0.7 |
| 190 | 0.97 | 0.4 | 0.4 | 0.6 |
| 210 | 0.98 | 0.3 | 0.4 | 0.5 |
| 230 | 0.98 | 0.3 | 0.3 | 0.4 |
| 250 | 0.99 | 0.3 | 0.2 | 0.3 |
| 270 | 0.99 | 0.2 | 0.2 | 0.3 |
| 300 | 0.99 | 0.2 | 0.2 | 0.3 |
| 340 | 1.00 | 0.2 | 0.2 | 0.2 |
| 380 | 1.00 | 0.1 | 0.1 | 0.2 |

**Acknowledgments** We congratulate our colleagues in the CERN accelerator departments for the excellent performance of the LHC and thank the technical and administrative staffs at CERN and at other CMS institutes for their contributions to the success of the CMS effort. In addition, we gratefully acknowledge the computing centres and personnel of the Worldwide LHC Computing Grid for delivering so effectively the computing infrastructure essential to our analyses. Finally, we acknowledge the enduring support for the construction and operation of the LHC and the CMS detector provided by the following funding agencies: BMWFW and FWF (Austria); FNRS and FWO (Belgium); CNPq, CAPES, FAPERJ, and FAPESP (Brazil); MES (Bulgaria); CERN; CAS, MoST, and NSFC (China); COLCIENCIAS (Colombia); MSES and CSF (Croatia); RPF (Cyprus); MoER, SF0690030s09 and ERDF (Estonia); Academy of Finland, MEC, and HIP (Finland); CEA and CNRS/IN2P3 (France); BMBF, DFG, and HGF (Germany); GSRT (Greece); OTKA and NIH (Hungary); DAE and DST (India); IPM (Iran); SFI (Ireland); INFN (Italy); NRF and WCU (Republic of Korea); LAS (Lithuania); MOE and UM (Malaysia); CINVESTAV, CONACYT, SEP, and UASLP-FAI (Mexico); MBIE (New Zealand); PAEC (Pakistan); MSHE and NSC (Poland); FCT (Portugal); JINR (Dubna); MON, RosAtom, RAS and RFBR (Russia); MESTD (Serbia); SEIDI and CPAN (Spain); Swiss Funding Agencies (Switzerland); MST (Taipei); ThEPCenter, IPST, STAR and NSTDA (Thailand); TUBITAK and TAEK (Turkey); NASU and SFFR (Ukraine); STFC (United Kingdom); DOE and NSF (USA). Individuals have received support from the Marie-Curie programme and the European Research Council and EPLANET (European Union); the Leventis Foundation; the A. P. Sloan Foundation; the Alexander von Humboldt Foundation; the Belgian Federal Science Policy Office; the Fonds pour la Formation à la Recherche dans l'Industrie et dans l'Agriculture (FRIA-Belgium); the Agentschap voor Innovatie door Wetenschap en Technologie (IWT-Belgium); the Ministry of Education, Youth and Sports (MEYS) of Czech Republic; the Council of Science and Industrial Research, India; the Compagnia di San Paolo (Torino); the HOMING PLUS programme of Foundation for Polish Science, cofinanced by EU, Regional Development Fund; and the Thalis and Aristeia programmes cofinanced by EU-ESF and the Greek NSRF.



## References

1. S. Dittmaier, P. Uwer, S. Weinzierl, NLO QCD corrections to $t\bar{t}$ + jet production at hadron colliders. Phys. Rev. Lett. **98**, 262002 (2007). doi:10.1103/PhysRevLett.98.262002. arXiv:hep-ph/0703120
2. G. Bevilacqua, M. Czakon, C.G. Papadopoulos, M. Worek, Hadronic top-quark pair production in association with two jets at Next-to-Leading Order QCD. Phys. Rev. D **84**, 114017 (2011). doi:10.1103/PhysRevD.84.114017. arXiv:1108.2851
3. M.I. Gresham, I.-W. Kim, K.M. Zurek, Searching for top flavor violating resonances. Phys. Rev. D **84**, 034025 (2011). doi:10.1103/PhysRevD.84.034025. arXiv:1102.0018
4. CMS Collaboration, The CMS experiment at the CERN LHC. JINST **3**, S08004 (2008). doi:10.1088/1748-0221/3/08/S08004
5. CMS Collaboration, Measurement of differential top-quark-pair production cross sections in pp collisions at $\sqrt{s} = 7$TeV. Eur. Phys. J. C **73**, 2339 (2013). doi:10.1140/epjc/s10052-013-2339-4. arXiv:hep-ex/1211.2220
6. ATLAS Collaboration, Measurement of $t\bar{t}$ production with a veto on additional central jet activity in pp collisions at $\sqrt{s} = 7$ TeV using the ATLAS detector. Eur. Phys. J. C **72** 2043 (2012). doi:10.1140/epjc/s10052-012-2043-9. arXiv:1203.5015

7. J. Alwall et al., The automated computation of tree-level and next-to-leading order differential cross sections, and their matching to parton shower simulations. JHEP **07**, 079 (2014). doi:10.1007/JHEP07(2014)079
8. T. Sjöstrand, S. Mrenna, P.Z. Skands, PYTHIA 6.4 physics and manual. JHEP **05** 026 (2006). doi:10.1088/1126-6708/2006/05/026. arXiv:hep-ph/0603175
9. M.L. Mangano, M. Moretti, F. Piccinini, M. Treccani, Matching matrix elements and shower evolution for top-quark production in hadronic collisions. JHEP **01**, 013 (2007). doi:10.1088/1126-6708/2007/01/013. arXiv:hep-ph/0611129
10. CMS Collaboration, Measurement of the underlying event activity at the LHC with $\sqrt{s} = 7$ TeV and comparison with $\sqrt{s} = 0.9$ TeV. JHEP **09**, 109 (2011). doi:10.1007/JHEP09(2011)109. arXiv:1107.0330
11. J. Pumplin et al., New generation of parton distributions with uncertainties from global QCD analysis. JHEP **07**, 012 (2002). doi:10.1088/1126-6708/2002/07/012. arXiv:hep-ph/0201195
12. P. Nason, A New method for combining NLO QCD with shower Monte Carlo algorithms. JHEP **11**, 040 (2004). doi:10.1088/1126-6708/2004/11/040. arXiv:hep-ph/0409146
13. S. Frixione, P. Nason, C. Oleari, Matching NLO QCD computations with Parton Shower simulations: the POWHEG method. JHEP **11**, 070 (2007). doi:10.1088/1126-6708/2007/11/070. arXiv:0709.2092
14. S. Alioli, P. Nason, C. Oleari, E. Re, NLO single-top production matched with shower in POWHEG: $s$- and $t$-channel contributions. JHEP **09**, 111 (2009). doi:10.1088/1126-6708/2009/09/111. arXiv:0907.4076. [Erratum doi:10.1007/JHEP02(2010)011]
15. E. Re, Single-top $Wt$-channel production matched with parton showers using the POWHEGmethod. Eur. Phys. J. C **71**, 1547 (2011). doi:10.1140/epjc/s10052-011-1547-z. arXiv:1009.2450
16. S. Frixione, B.R. Webber, Matching NLO QCD computations and parton shower simulations. JHEP **06**, 29 (2002). doi:10.1088/1126-6708/2002/06/029. arXiv:hep-ph/0204244
17. G. Corcella et al., HERWIG 6: an event generator for hadron emission reactions with interfering gluons (including supersymmetric processes). JHEP **01**, 010 (2001). doi:10.1088/1126-6708/2001/01/010. arXiv:hep-ph/0011363
18. N. Kidonakis, NNLL resummation for s-channel single top quark production. Phys. Rev. D **81**, 054028 (2010). doi:10.1103/PhysRevD.81.054028. arXiv:1001.5034
19. N. Kidonakis, Next-to-next-to-leading-order collinear and soft gluon corrections for t-channel single top quark production. Phys. Rev. D **83**, 091503 (2011). doi:10.1103/PhysRevD.83.091503. arXiv:1103.2792
20. N. Kidonakis, Two-loop soft anomalous dimensions for single top quark associated production with $W^-$ or $H^-$. Phys. Rev. D **82**, 054018 (2010). doi:10.1103/PhysRevD.82.054018. arXiv:hep-ph/1005.4451
21. J.M. Campbell, R.K. Ellis, C. Williams, Vector boson pair production at the LHC. JHEP **07**, 018 (2011). doi:10.1007/JHEP07(2011)018. arXiv:1105.0020
22. M. Czakon, A. Mitov, Top++: a program for the calculation of the top-pair cross-section at hadron colliders (2011). arXiv:1112.5675
23. S. Alekhin et al., The PDF4LHC Working Group Interim Report (2011). arXiv:1101.0536
24. M. Botje et al., The PDF4LHC Working Group Interim Recommendations. (2011). arXiv:1101.0538
25. A.D. Martin, W.J. Stirling, R.S. Thorne, G. Watt, Parton distributions for the LHC. Eur. Phys. J. C **63**, 189 (2009). doi:10.1140/epjc/s10052-009-1072-5. arXiv:0901.0002
26. H.-L. Lai et al., New parton distributions for collider physics. Phys. Rev. D **82**, 074024 (2010). doi:10.1103/PhysRevD.82.074024. arXiv:1007.2241
27. J. Gao et al., CT10 next-to-next-to-leading order global analysis of QCD. Phys. Rev. D **89**, 033009 (2014). doi:10.1103/PhysRevD.89.033009. arXiv:1302.6246
28. NNPDF Collaboration, Parton distributions with LHC data. Nucl. Phys. B **867**, 244 (2013). doi:10.1016/j.nuclphysb.2012.10.003 arXiv:1207.1303
29. Nucl. Instrum. Meth. A GEANT4—a simulation toolkit. **506**, 250 (2003). doi:10.1016/S0168-9002(03)01368-8
30. CMS Collaboration, Particle-Flow Event Reconstruction in CMS and Performance for Jets, Taus, and $E_{\mathrm{T}}^{\mathrm{miss}}$. CMS Physics Analysis Summary CMS-PAS-PFT-09-001 (2009). http://cdsweb.cern.ch/record/1194487
31. CMS Collaboration, Commissioning of the Particle-Flow Reconstruction in Minimum-Bias and Jet Events from PP Collisions at 7 TeV. CMS Physics Analysis Summary CMS-PAS-PFT-10-002 (2010). http://cdsweb.cern.ch/record/1279341
32. M. Cacciari, G.P. Salam, G. Soyez, The catchment area of jets. JHEP **04**, 005 (2008). doi:10.1088/1126-6708/2008/04/005. arXiv:0802.1188
33. CMS Collaboration, Electron Reconstruction and Identification at $\sqrt{s} = 7$ TeV. CMS Physics Analysis Summary CMS-PAS-EGM-10-004 (2010). http://cdsweb.cern.ch/record/1299116
34. CMS Collaboration, Performance of CMS muon reconstruction in pp collision events at $\sqrt{s} = 7$ TeV. JINST **7**, P10002 (2012). doi:10.1088/1748-0221/7/10/P10002. arXiv:1206.4071
35. CMS Collaboration, Determination of jet energy calibration and transverse momentum resolution in CMS. JINST **6**, P11002 (2011). doi:10.1088/1748-0221/6/11/P11002. arXiv:1107.4277
36. M. Cacciari, G.P. Salam, Dispelling the $N^3$ myth for the $k_t$ jet-finder. Phys. Lett. B **641**, 57 (2006). doi:10.1016/j.physletb.2006.08.037. arXiv:hep-ph/0512210
37. M. Cacciari, G.P. Salam, G. Soyez, The anti-$k_t$ jet clustering algorithm. JHEP **04**, 063 (2008). doi:10.1088/1126-6708/2008/04/063. arXiv:0802.1189
38. M. Cacciari, G. P. Salam, and G. Soyez, "FastJet user manual", (2011). arXiv:1111.6097.
39. CMS Collaboration, Identification of b-quark jets with the CMS experiment. JINST **08**, P04013 (2013). doi:10.1088/1748-0221/8/04/P04013. arXiv:1211.4462
40. Particle Data Group, J. Beringer et al., Review of particle physics. Phys. Rev. D **86**, 010001 (2012). doi:10.1103/PhysRevD.86.010001
41. CMS Collaboration, Measurement of the $t\bar{t}$ production cross section and the top quark mass in the dilepton channel in pp collisions at $\sqrt{s} = 7$ TeV. JHEP **07**, 049 (2011). doi:10.1007/JHEP07(2011)049. arXiv:1105.5661
42. CMS Collaboration, Measurement of the electron charge asymmetry in inclusive $W$ production in pp collisions at $\sqrt{s} = 7$ TeV. Phys. Rev. Lett. **109**, 111806 (2012). doi:10.1103/PhysRevLett.109.111806. arXiv:1206.2598
43. CMS Collaboration, Measurement of the $t\bar{t}$ production cross section in pp collisions at $\sqrt{s} = 7$ TeV with lepton + jets final states. Phys. Lett. B **720**, 83 (2013). doi:10.1016/j.physletb.2013.02.021. arXiv:1212.6682
44. CMS Collaboration, Jet Energy Resolution in CMS at $\sqrt{s} = 7$ TeV. CMS Physics Analysis Summary CMS-PAS-JME-10-014 (2010). http://cdsweb.cern.ch/record/1299116
45. P.Z. Skands, D. Wicke, Non-perturbative QCD effects and the top mass at the Tevatron. Eur. Phys. J. C **52**, 133 (2007). doi:10.1140/epjc/s10052-007-0352-1. arXiv:hep-ph/0703081
46. P.Z. Skands, Tuning Monte Carlo generators: The Perugia tunes. Phys. Rev. D **82**, 074018 (2010). doi:10.1103/PhysRevD.82.074018. arXiv:1005.3457

47. CMS Collaboration, Measurement of the $t\bar{t}$ production cross section in pp collisions at $\sqrt{s} = 7$TeV using the kinematic properties of events with leptons and jets. Eur. Phys. J. C **71**, 1721 (2011). doi:10.1140/epjc/s10052-011-1721-3. arXiv:1106.0902
48. CMS Collaboration, Measurement of the $t\bar{t}$ production cross section in the dilepton channel in pp collisions at $\sqrt{s} = 7$ TeV. JHEP **11**, 067 (2012). doi:10.1007/JHEP11(2012)067. arXiv:1208.2671
49. CMS Collaboration, Absolute Calibration of the Luminosity Measurement at CMS: Winter 2012 Update. CMS Physics Analysis Summary CMS-PAS-SMP-12-008 (2012). http://cdsweb.cern.ch/record/1434360
50. A. Höcker, V. Kartvelishvili, SVD approach to data unfolding. Nucl. Instrum. Meth. A **372**, 469 (1996). doi:10.1016/0168-9002(95)01478-0. arXiv:hep-ph/9509307
51. V. Blobel, "An unfolding method for high energy physics experiments", (2002). arXiv:hep-ex/0208022
52. F. James, *Statistical Methods in Experimental Physics*, 2nd edn. World (Scientific, Singapore, 2006)

## The CMS Collaboration

**Yerevan Physics Institute, Yerevan, Armenia**
S. Chatrchyan, V. Khachatryan, A. M. Sirunyan, A. Tumasyan

**Institut für Hochenergiephysik der OeAW, Wien, Austria**
W. Adam, T. Bergauer, M. Dragicevic, J. Erö, C. Fabjan[1], M. Friedl, R. Frühwirth[1], V. M. Ghete, C. Hartl, N. Hörmann, J. Hrubec, M. Jeitler[1], W. Kiesenhofer, V. Knünz, M. Krammer[1], I. Krätschmer, D. Liko, I. Mikulec, D. Rabady[2], B. Rahbaran, H. Rohringer, R. Schöfbeck, J. Strauss, A. Taurok, W. Treberer-Treberspurg, W. Waltenberger, C.-E. Wulz[1]

**National Centre for Particle and High Energy Physics, Minsk, Belarus**
V. Mossolov, N. Shumeiko, J. Suarez Gonzalez

**Universiteit Antwerpen, Antwerpen, Belgium**
S. Alderweireldt, M. Bansal, S. Bansal, T. Cornelis, E. A. De Wolf, X. Janssen, A. Knutsson, S. Luyckx, S. Ochesanu, B. Roland, R. Rougny, H. Van Haevermaet, P. Van Mechelen, N. Van Remortel, A. Van Spilbeeck

**Vrije Universiteit Brussel, Brussel, Belgium**
F. Blekman, S. Blyweert, J. D'Hondt, N. Heracleous, A. Kalogeropoulos, J. Keaveney, T. J. Kim, S. Lowette, M. Maes, A. Olbrechts, D. Strom, S. Tavernier, W. Van Doninck, P. Van Mulders, G. P. Van Onsem, I. Villella

**Université Libre de Bruxelles, Bruxelles, Belgium**
C. Caillol, B. Clerbaux, G. De Lentdecker, L. Favart, A. P. R. Gay, A. Léonard, P. E. Marage, A. Mohammadi, L. Perniè, T. Reis, T. Seva, L. Thomas, C. Vander Velde, P. Vanlaer, J. Wang

**Ghent University, Ghent, Belgium**
V. Adler, K. Beernaert, L. Benucci, A. Cimmino, S. Costantini, S. Crucy, S. Dildick, G. Garcia, B. Klein, J. Lellouch, J. Mccartin, A. A. Ocampo Rios, D. Ryckbosch, S. Salva Diblen, M. Sigamani, N. Strobbe, F. Thyssen, M. Tytgat, S. Walsh, E. Yazgan, N. Zaganidis

**Université Catholique de Louvain, Louvain-la-Neuve, Belgium**
S. Basegmez, C. Beluffi[3], G. Bruno, R. Castello, A. Caudron, L. Ceard, G. G. Da Silveira, C. Delaere, T. du Pree, D. Favart, L. Forthomme, A. Giammanco[4], J. Hollar, P. Jez, M. Komm, V. Lemaitre, J. Liao, O. Militaru, C. Nuttens, D. Pagano, A. Pin, K. Piotrzkowski, A. Popov[5], L. Quertenmont, M. Selvaggi, M. Vidal Marono, J. M. Vizan Garcia

**Université de Mons, Mons, Belgium**
N. Beliy, T. Caebergs, E. Daubie, G. H. Hammad

**Centro Brasileiro de Pesquisas Fisicas, Rio de Janeiro, Brazil**
G. A. Alves, M. Correa Martins Junior, T. Martins, M. E. Pol, M. H. G. Souza

**Universidade do Estado do Rio de Janeiro, Rio de Janeiro, Brazil**
W. L. Aldá Júnior, W. Carvalho, J. Chinellato[6], A. Custódio, E. M. Da Costa, D. De Jesus Damiao, C. De Oliveira Martins, S. Fonseca De Souza, H. Malbouisson, M. Malek, D. Matos Figueiredo, L. Mundim, H. Nogima, W. L. Prado Da Silva, J. Santaolalla, A. Santoro, A. Sznajder, E. J. Tonelli Manganote[6], A. Vilela Pereira

**Universidade Estadual Paulista [a], Universidade Federal do ABC [b], São Paulo, Brazil**
C. A. Bernardes[b], F. A. Dias[a,7], T. R. Fernandez Perez Tomei[a], E. M. Gregores[b], P. G. Mercadante[b], S. F. Novaes[a], Sandra S. Padula[a]

**Institute for Nuclear Research and Nuclear Energy, Sofia, Bulgaria**
V. Genchev[2], P. Iaydjiev[2], A. Marinov, S. Piperov, M. Rodozov, G. Sultanov, M. Vutova

**University of Sofia, Sofia, Bulgaria**
A. Dimitrov, I. Glushkov, R. Hadjiiska, V. Kozhuharov, L. Litov, B. Pavlov, P. Petkov

**Institute of High Energy Physics, Beijing, China**
J. G. Bian, G. M. Chen, H. S. Chen, M. Chen, R. Du, C. H. Jiang, D. Liang, S. Liang, X. Meng, R. Plestina[8], J. Tao, X. Wang, Z. Wang

**State Key Laboratory of Nuclear Physics and Technology, Peking University, Beijing, China**
C. Asawatangtrakuldee, Y. Ban, Y. Guo, Q. Li, W. Li, S. Liu, Y. Mao, S. J. Qian, D. Wang, L. Zhang, W. Zou

**Universidad de Los Andes, Bogotá, Colombia**
C. Avila, L. F. Chaparro Sierra, C. Florez, J. P. Gomez, B. Gomez Moreno, J. C. Sanabria

**Technical University of Split, Split, Croatia**
N. Godinovic, D. Lelas, D. Polic, I. Puljak

**University of Split, Split, Croatia**
Z. Antunovic, M. Kovac

**Institute Rudjer Boskovic, Zagreb, Croatia**
V. Brigljevic, K. Kadija, J. Luetic, D. Mekterovic, S. Morovic, L. Tikvica

**University of Cyprus, Nicosia, Cyprus**
A. Attikis, G. Mavromanolakis, J. Mousa, C. Nicolaou, F. Ptochos, P. A. Razis

**Charles University, Prague, Czech Republic**
M. Finger, M. Finger Jr.

**Academy of Scientific Research and Technology of the Arab Republic of Egypt, Egyptian Network of High Energy Physics, Cairo, Egypt**
Y. Assran[9], S. Elgammal[10], A. Ellithi Kamel[11], M. A. Mahmoud[12], A. Mahrous[13], A. Radi[14,15]

**National Institute of Chemical Physics and Biophysics, Tallinn, Estonia**
M. Kadastik, M. Müntel, M. Murumaa, M. Raidal, A. Tiko

**Department of Physics, University of Helsinki, Helsinki, Finland**
P. Eerola, G. Fedi, M. Voutilainen

**Helsinki Institute of Physics, Helsinki, Finland**
J. Härkönen, V. Karimäki, R. Kinnunen, M. J. Kortelainen, T. Lampén, K. Lassila-Perini, S. Lehti, T. Lindén, P. Luukka, T. Mäenpää, T. Peltola, E. Tuominen, J. Tuominiemi, E. Tuovinen, L. Wendland

**Lappeenranta University of Technology, Lappeenranta, Finland**
T. Tuuva

**DSM/IRFU, CEA/Saclay, Gif-sur-Yvette, France**
M. Besancon, F. Couderc, M. Dejardin, D. Denegri, B. Fabbro, J. L. Faure, F. Ferri, S. Ganjour, A. Givernaud, P. Gras, G. Hamel de Monchenault, P. Jarry, E. Locci, J. Malcles, A. Nayak, J. Rander, A. Rosowsky, M. Titov

**Laboratoire Leprince-Ringuet, Ecole Polytechnique, IN2P3-CNRS, Palaiseau, France**
S. Baffioni, F. Beaudette, P. Busson, C. Charlot, N. Daci, T. Dahms, M. Dalchenko, L. Dobrzynski, N. Filipovic, A. Florent, R. Granier de Cassagnac, L. Mastrolorenzo, P. Miné, C. Mironov, I. N. Naranjo, M. Nguyen, C. Ochando, P. Paganini, D. Sabes, R. Salerno, J. b. Sauvan, Y. Sirois, C. Veelken, Y. Yilmaz, A. Zabi

**Institut Pluridisciplinaire Hubert Curien, Université de Strasbourg, Université de Haute Alsace Mulhouse, CNRS/IN2P3, Strasbourg, France**
J.-L. Agram[16], J. Andrea, D. Bloch, J.-M. Brom, E. C. Chabert, C. Collard, E. Conte[16], F. Drouhin[16], J.-C. Fontaine[16], D. Gelé, U. Goerlach, C. Goetzmann, P. Juillot, A.-C. Le Bihan, P. Van Hove

**Centre de Calcul de l'Institut National de Physique Nucleaire et de Physique des Particules, CNRS/IN2P3, Villeurbanne, France**
S. Gadrat

**Institut de Physique Nucléaire de Lyon, Université de Lyon, Université Claude Bernard Lyon 1, CNRS-IN2P3, Villeurbanne, France**
S. Beauceron, N. Beaupere, G. Boudoul, S. Brochet, C. A. Carrillo Montoya, J. Chasserat, R. Chierici, D. Contardo[2], P. Depasse, H. El Mamouni, J. Fan, J. Fay, S. Gascon, M. Gouzevitch, B. Ille, T. Kurca, M. Lethuillier, L. Mirabito, S. Perries, J. D. Ruiz Alvarez, L. Sgandurra, V. Sordini, M. Vander Donckt, P. Verdier, S. Viret, H. Xiao

**Institute of High Energy Physics and Informatization, Tbilisi State University, Tbilisi, Georgia**
Z. Tsamalaidze[17]

**RWTH Aachen University, I. Physikalisches Institut, Aachen, Germany**
C. Autermann, S. Beranek, M. Bontenackels, B. Calpas, M. Edelhoff, L. Feld, O. Hindrichs, K. Klein, A. Ostapchuk, A. Perieanu, F. Raupach, J. Sammet, S. Schael, D. Sprenger, H. Weber, B. Wittmer, V. Zhukov[5]

**RWTH Aachen University, III. Physikalisches Institut A, Aachen, Germany**
M. Ata, J. Caudron, E. Dietz-Laursonn, D. Duchardt, M. Erdmann, R. Fischer, A. Güth, T. Hebbeker, C. Heidemann, K. Hoepfner, D. Klingebiel, S. Knutzen, P. Kreuzer, M. Merschmeyer, A. Meyer, M. Olschewski, K. Padeken, P. Papacz, H. Reithler, S. A. Schmitz, L. Sonnenschein, D. Teyssier, S. Thüer, M. Weber

**RWTH Aachen University, III. Physikalisches Institut B, Aachen, Germany**
V. Cherepanov, Y. Erdogan, G. Flügge, H. Geenen, M. Geisler, W. Haj Ahmad, F. Hoehle, B. Kargoll, T. Kress, Y. Kuessel, J. Lingemann[2], A. Nowack, I. M. Nugent, L. Perchalla, O. Pooth, A. Stahl

**Deutsches Elektronen-Synchrotron, Hamburg, Germany**
I. Asin, N. Bartosik, J. Behr, W. Behrenhoff, U. Behrens, A. J. Bell, M. Bergholz[18], A. Bethani, K. Borras, A. Burgmeier, A. Cakir, L. Calligaris, A. Campbell, S. Choudhury, F. Costanza, C. Diez Pardos, S. Dooling, T. Dorland, G. Eckerlin, D. Eckstein, T. Eichhorn, G. Flucke, A. Geiser, A. Grebenyuk, P. Gunnellini, S. Habib, J. Hauk, G. Hellwig, M. Hempel, D. Horton, H. Jung, M. Kasemann, P. Katsas, J. Kieseler, C. Kleinwort, M. Krämer, D. Krücker, W. Lange, J. Leonard, K. Lipka, W. Lohmann[18], B. Lutz, R. Mankel, I. Marfin, I.-A. Melzer-Pellmann, A. B. Meyer, J. Mnich, A. Mussgiller, S. Naumann-Emme, O. Novgorodova, F. Nowak, E. Ntomari, H. Perrey, A. Petrukhin, D. Pitzl, R. Placakyte, A. Raspereza, P. M. Ribeiro Cipriano, C. Riedl, E. Ron, M. Ö. Sahin, J. Salfeld-Nebgen, P. Saxena, R. Schmidt[18], T. Schoerner-Sadenius, M. Schröder, M. Stein, A. D. R. Vargas Trevino, R. Walsh, C. Wissing

**University of Hamburg, Hamburg, Germany**
M. Aldaya Martin, V. Blobel, H. Enderle, J. Erfle, E. Garutti, K. Goebel, M. Görner, M. Gosselink, J. Haller, R. S. Höing, H. Kirschenmann, R. Klanner, R. Kogler, J. Lange, T. Lapsien, T. Lenz, I. Marchesini, J. Ott, T. Peiffer, N. Pietsch, D. Rathjens, C. Sander, H. Schettler, P. Schleper, E. Schlieckau, A. Schmidt, M. Seidel, J. Sibille[19], V. Sola, H. Stadie, G. Steinbrück, D. Troendle, E. Usai, L. Vanelderen

**Institut für Experimentelle Kernphysik, Karlsruhe, Germany**
C. Barth, C. Baus, J. Berger, C. Böser, E. Butz, T. Chwalek, W. De Boer, A. Descroix, A. Dierlamm, M. Feindt, M. Guthoff[2], F. Hartmann[2], T. Hauth[2], H. Held, K. H. Hoffmann, U. Husemann, I. Katkov[5], A. Kornmayer[2], E. Kuznetsova, P. Lobelle Pardo, D. Martschei, H. Mildner, M. U. Mozer, Th. Müller, M. Niegel, A. Nürnberg, O. Oberst, G. Quast, K. Rabbertz, F. Ratnikov, S. Röcker, F.-P. Schilling, G. Schott, H. J. Simonis, F. M. Stober, R. Ulrich, J. Wagner-Kuhr, S. Wayand, T. Weiler, S. Williamson, R. Wolf, M. Zeise

**Institute of Nuclear and Particle Physics (INPP), NCSR Demokritos, Aghia Paraskevi, Greece**
G. Anagnostou, G. Daskalakis, T. Geralis, V. A. Giakoumopoulou, S. Kesisoglou, A. Kyriakis, D. Loukas, A. Markou, C. Markou, A. Psallidas, I. Topsis-Giotis

**University of Athens, Athens, Greece**
L. Gouskos, A. Panagiotou, N. Saoulidou, E. Stiliaris

**University of Ioánnina, Ioannina, Greece**
X. Aslanoglou, I. Evangelou[2], G. Flouris, C. Foudas[2], J. Jones, P. Kokkas, N. Manthos, I. Papadopoulos, E. Paradas

**Wigner Research Centre for Physics, Budapest, Hungary**
G. Bencze[2], C. Hajdu, P. Hidas, D. Horvath[20], F. Sikler, V. Veszpremi, G. Vesztergombi[21], A. J. Zsigmond

**Institute of Nuclear Research ATOMKI, Debrecen, Hungary**
N. Beni, S. Czellar, J. Molnar, J. Palinkas, Z. Szillasi

**University of Debrecen, Debrecen, Hungary**
J. Karancsi, P. Raics, Z. L. Trocsanyi, B. Ujvari

**National Institute of Science Education and Research, Bhubaneswar, India**
S. K. Swain

**Panjab University, Chandigarh, India**
S. B. Beri, V. Bhatnagar, N. Dhingra, R. Gupta, M. Kaur, M. Mittal, N. Nishu, A. Sharma, J. B. Singh

**University of Delhi, Delhi, India**
Ashok Kumar, Arun Kumar, S. Ahuja, A. Bhardwaj, B. C. Choudhary, A. Kumar, S. Malhotra, M. Naimuddin, K. Ranjan, V. Sharma, R. K. Shivpuri

**Saha Institute of Nuclear Physics, Kolkata, India**
S. Banerjee, S. Bhattacharya, K. Chatterjee, S. Dutta, B. Gomber, Sa. Jain, Sh. Jain, R. Khurana, A. Modak, S. Mukherjee, D. Roy, S. Sarkar, M. Sharan, A. P. Singh

**Bhabha Atomic Research Centre, Mumbai, India**
A. Abdulsalam, D. Dutta, S. Kailas, V. Kumar, A. K. Mohanty[2], L. M. Pant, P. Shukla, A. Topkar

**Tata Institute of Fundamental Research - EHEP, Mumbai, India**
T. Aziz, R. M. Chatterjee, S. Ganguly, S. Ghosh, M. Guchait[22], A. Gurtu[23], G. Kole, S. Kumar, M. Maity[24], G. Majumder, K. Mazumdar, G.B. Mohanty, B. Parida, K. Sudhakar, N. Wickramage[25]

**Tata Institute of Fundamental Research - HECR, Mumbai, India**
S. Banerjee, R. K. Dewanjee, S. Dugad

**Institute for Research in Fundamental Sciences (IPM), Tehran, Iran**
H. Arfaei, H. Bakhshiansohi, H. Behnamian, S. M. Etesami[26], A. Fahim[27], A. Jafari, M. Khakzad, M. Mohammadi Najafabadi, M. Naseri, S. Paktinat Mehdiabadi, B. Safarzadeh[28], M. Zeinali

**University College Dublin, Dublin, Ireland**
M. Grunewald

**INFN Sezione di Bari [a], Università di Bari [b], Politecnico di Bari [c], Bari, Italy**
M. Abbrescia[a,b], L. Barbone[a,b], C. Calabria[a,b], S. S. Chhibra[a,b], A. Colaleo[a], D. Creanza[a,c], N. De Filippis[a,c], M. De Palma[a,b], L. Fiore[a], G. Iaselli[a,c], G. Maggi[a,c], M. Maggi[a], B. Marangelli[a,b], S. My[a,c], S. Nuzzo[a,b], N. Pacifico[a], A. Pompili[a,b], G. Pugliese[a,c], R. Radogna[a,b], G. Selvaggi[a,b], L. Silvestris[a], G. Singh[a,b], R. Venditti[a,b], P. Verwilligen[a], G. Zito[a]

**INFN Sezione di Bologna [a], Università di Bologna [b], Bologna, Italy**
G. Abbiendi[a], A. C. Benvenuti[a], D. Bonacorsi[a,b], S. Braibant-Giacomelli[a,b], L. Brigliadori[a,b], R. Campanini[a,b], P. Capiluppi[a,b], A. Castro[a,b], F. R. Cavallo[a], G. Codispoti[a,b], M. Cuffiani[a,b], G. M. Dallavalle[a], F. Fabbri[a], A. Fanfani[a,b], D. Fasanella[a,b], P. Giacomelli[a], C. Grandi[a], L. Guiducci[a,b], S. Marcellini[a], G. Masetti[a], M. Meneghelli[a,b], A. Montanari[a], F. L. Navarria[a,b], F. Odorici[a], A. Perrotta[a], F. Primavera[a,b], A. M. Rossi[a,b], T. Rovelli[a,b], G. P. Siroli[a,b], N. Tosi[a,b], R. Travaglini[a,b]

**INFN Sezione di Catania [a], Università di Catania [b], CSFNSM [c], Catania, Italy**
S. Albergo[a,b], G. Cappello[a], M. Chiorboli[a,b], S. Costa[a,b], F. Giordano[a,2], R. Potenza[a,b], A. Tricomi[a,b], C. Tuve[a,b]

**INFN Sezione di Firenze [a], Università di Firenze [b], Florence, Italy**
G. Barbagli[a], V. Ciulli[a,b], C. Civinini[a], R. D'Alessandro[a,b],E. Focardi[a,b], E. Gallo[a], S. Gonzi[a,b], V. Gori[a,b], P. Lenzi[a,b], M. Meschini[a], S. Paoletti[a], G. Sguazzoni[a], A. Tropiano[a,b]

**INFN Laboratori Nazionali di Frascati, Frascati, Italy**
L. Benussi, S. Bianco, F. Fabbri, D. Piccolo

**INFN Sezione di Genova [a], Università di Genova [b], Genoa, Italy**
P. Fabbricatore[a], F. Ferro[a], M. Lo Vetere[a,b], R. Musenich[a], E. Robutti[a], S. Tosi[a,b]

**INFN Sezione di Milano-Bicocca [a], Università di Milano-Bicocca [b], Milan, Italy**
M. E. Dinardo[a,b], S. Fiorendi[a,b,2], S. Gennai[a], R. Gerosa, A. Ghezzi[a,b], P. Govoni[a,b], M. T. Lucchini[a,b,2], S. Malvezzi[a], R. A. Manzoni[a,b,2], A. Martelli[a,b,2], B. Marzocchi, D. Menasce[a], L. Moroni[a], M. Paganoni[a,b], D. Pedrini[a], S. Ragazzi[a,b], N. Redaelli[a], T. Tabarelli de Fatis[a,b]

**INFN Sezione di Napoli [a], Università di Napoli 'Federico II' [b], Università della Basilicata (Potenza) [c], Università G. Marconi (Roma) [d], Naples, Italy**
S. Buontempo[a], N. Cavallo[a,c], S. Di Guida[a,d], F. Fabozzi[a,c],A. O. M. Iorio[a,b], L. Lista[a], S. Meola[a,d,2], M. Merola[a], P. Paolucci[a,2]

**INFN Sezione di Padova [a], Università di Padova [b], Università di Trento (Trento) [c], Padua, Italy**
P. Azzi[a], N. Bacchetta[a], M. Biasotto[a,29], A. Branca[a,b], T. Dorigo[a], U. Dosselli[a], F. Fanzago[a], M. Galanti[a,b,2], F. Gasparini[a,b], P. Giubilato[a,b], A. Gozzelino[a], M. Gulmini[a,29], K. Kanishchev[a,c], S. Lacaprara[a], I. Lazzizzera[a,c], M. Margoni[a,b], G. Maron[a,29], A. T. Meneguzzo[a,b], M. Michelotto[a], J. Pazzini[a,b], N. Pozzobon[a,b], P. Ronchese[a,b], M. Sgaravatto[a], F. Simonetto[a,b], E. Torassa[a], M. Tosi[a,b], P. Zotto[a,b], A. Zucchetta[a,b], G. Zumerle[a,b]

**INFN Sezione di Pavia [a], Università di Pavia [b], Pavia, Italy**
M. Gabusi[a,b], S. P. Ratti[a,b], C. Riccardi[a,b], P. Salvini[a], P. Vitulo[a,b]

**INFN Sezione di Perugia [a], Università di Perugia [b], Perugia, Italy**
M. Biasini[a,b], G. M. Bilei[a], L. Fanò[a,b], P. Lariccia[a,b], G. Mantovani[a,b], M. Menichelli[a], F. Romeo[a,b], A. Saha[a], A. Santocchia[a,b], A. Spiezia[a,b]

**INFN Sezione di Pisa [a], Università di Pisa [b], Scuola Normale Superiore di Pisa [c], Pisa, Italy**
K. Androsov[a,30], P. Azzurri[a], G. Bagliesi[a], J. Bernardini[a], T. Boccali[a], G. Broccolo[a,c], R. Castaldi[a], M. A. Ciocci[a,30], R. Dell'Orso[a], S. Donato[a,c], F. Fiori[a,c], L. Foà[a,c], A. Giassi[a], M. T. Grippo[a,30], A. Kraan[a], F. Ligabue[a,c], T. Lomtadze[a], L. Martini[a,b], A. Messineo[a,b], C. S. Moon[a,31], F. Palla[a,2], A. Rizzi[a,b], A. Savoy-Navarro[a,32], A. T. Serban[a], P. Spagnolo[a], P. Squillacioti[a,30], R. Tenchini[a], G. Tonelli[a,b], A. Venturi[a], P. G. Verdini[a], C. Vernieri[a,c]

**INFN Sezione di Roma [a], Università di Roma [b], Rome, Italy**
L. Barone[a,b], F. Cavallari[a], D. Del Re[a,b], M. Diemoz[a], M. Grassi[a,b], C. Jorda[a], E. Longo[a,b], F. Margaroli[a,b], P. Meridiani[a], F. Micheli[a,b], S. Nourbakhsh[a,b], G. Organtini[a,b], R. Paramatti[a], S. Rahatlou[a,b], C. Rovelli[a], L. Soffi[a,b], P. Traczyk[a,b]

**INFN Sezione di Torino [a], Università di Torino [b], Università del Piemonte Orientale (Novara) [c], Turin, Italy**
N. Amapane[a,b], R. Arcidiacono[a,c], S. Argiro[a,b], M. Arneodo[a], R. Bellan[a,b], C. Biino[a], N. Cartiglia[a], S. Casasso[a,b], M. Costa[a,b], A. Degano[a,b], N. Demaria[a], C. Mariotti[a], S. Maselli[a], E. Migliore[a,b], V. Monaco[a,b], M. Musich[a], M. M. Obertino[a,c], G. Ortona[a,b], L. Pacher[a,b], N. Pastrone[a],M. Pelliccioni[a,2], G. L. Pinna Angioni[a,b], A. Potenza[a], A. Romero[a,b], M. Ruspa[a,c], R. Sacchi[a,b], A. Solano[a,b], A. Staiano[a], U. Tamponi[a]

**INFN Sezione di Trieste [a], Università di Trieste [b], Trieste, Italy**
S. Belforte[a], V. Candelise[a,b], M. Casarsa[a], F. Cossutti[a], G. Della Ricca[a,b], B. Gobbo[a], C. La Licata[a,b], M. Marone[a,b], D. Montanino[a,b], A. Schizzi[a,b], T. Umer[a,b], A. Zanetti[a]

**Kangwon National University, Chunchon, Korea**
S. Chang, T. Y. Kim, S. K. Nam

**Kyungpook National University, Taegu, Korea**
D. H. Kim, G. N. Kim, J. E. Kim, M. S. Kim, D. J. Kong, S. Lee, Y. D. Oh, H. Park, A. Sakharov, D. C. Son

**Chonnam National University, Institute for Universe and Elementary Particles, Kwangju, Korea**
J. Y. Kim, Zero J. Kim, S. Song

**Korea University, Seoul, Korea**
S. Choi, D. Gyun, B. Hong, M. Jo, H. Kim, Y. Kim, B. Lee, K. S. Lee, S. K. Park, Y. Roh

**University of Seoul, Seoul, Korea**
M. Choi, J. H. Kim, C. Park, I. C. Park, S. Park, G. Ryu

**Sungkyunkwan University, Suwon, Korea**
Y. Choi, Y. K. Choi, J. Goh, E. Kwon, J. Lee, H. Seo, I. Yu

**Vilnius University, Vilnius, Lithuania**
A. Juodagalvis

**National Centre for Particle Physics, Universiti Malaya, Kuala Lumpur, Malaysia**
J. R. Komaragiri

**Centro de Investigacion y de Estudios Avanzados del IPN, Mexico City, Mexico**
H. Castilla-Valdez, E. De La Cruz-Burelo, I. Heredia-de La Cruz[33], R. Lopez-Fernandez, J. Martínez-Ortega, A. Sanchez-Hernandez, L. M. Villasenor-Cendejas

**Universidad Iberoamericana, Mexico City, Mexico**
S. Carrillo Moreno, F. Vazquez Valencia

**Benemerita Universidad Autonoma de Puebla, Puebla, Mexico**
H. A. Salazar Ibarguen

**Universidad Autónoma de San Luis Potosí, San Luis Potosí, Mexico**
E. Casimiro Linares, A. Morelos Pineda

**University of Auckland, Auckland, New Zealand**
D. Krofcheck

**University of Canterbury, Christchurch, New Zealand**
P. H. Butler, R. Doesburg, S. Reucroft

**National Centre for Physics, Quaid-I-Azam University, Islamabad, Pakistan**
A. Ahmad, M. Ahmad, M. I. Asghar, J. Butt, Q. Hassan, H. R. Hoorani, W. A. Khan, T. Khurshid, S. Qazi, M. A. Shah, M. Shoaib

**National Centre for Nuclear Research, Swierk, Poland**
H. Bialkowska, M. Bluj[34], B. Boimska, T. Frueboes, M. Górski, M. Kazana, K. Nawrocki, K. Romanowska-Rybinska, M. Szleper, G. Wrochna, P. Zalewski

**Institute of Experimental Physics, Faculty of Physics, University of Warsaw, Warsaw, Poland**
G. Brona, K. Bunkowski, M. Cwiok, W. Dominik, K. Doroba, A. Kalinowski, M. Konecki, J. Krolikowski, M. Misiura, W. Wolszczak

**Laboratório de Instrumentação e Física Experimental de Partículas, Lisbon, Portugal**
P. Bargassa, C. Beirão Da Cruz E Silva, P. Faccioli, P. G. Ferreira Parracho, M. Gallinaro, F. Nguyen, J. Rodrigues Antunes, J. Seixas, J. Varela, P. Vischia

**Joint Institute for Nuclear Research, Dubna, Russia**
P. Bunin, M. Gavrilenko, I. Golutvin, A. Kamenev, V. Karjavin, V. Konoplyanikov, V. Korenkov, G. Kozlov, A. Lanev, V. Matveev[35], P. Moisenz, V. Palichik, V. Perelygin, S. Shmatov, S. Shulha, N. Skatchkov, V. Smirnov, A. Zarubin

**Petersburg Nuclear Physics Institute, Gatchina, St. Petersburg, Russia**
V. Golovtsov, Y. Ivanov, V. Kim[36], P. Levchenko, V. Murzin, V. Oreshkin, I. Smirnov, V. Sulimov, L. Uvarov, S. Vavilov, A. Vorobyev, An. Vorobyev

**Institute for Nuclear Research, Moscow, Russia**
Yu. Andreev, A. Dermenev, S. Gninenko, N. Golubev, M. Kirsanov, N. Krasnikov, A. Pashenkov, D. Tlisov, A. Toropin

**Institute for Theoretical and Experimental Physics, Moscow, Russia**
V. Epshteyn, V. Gavrilov, N. Lychkovskaya, V. Popov, G. Safronov, S. Semenov, A. Spiridonov, V. Stolin, E. Vlasov, A. Zhokin

**P.N. Lebedev Physical Institute, Moscow, Russia**
V. Andreev, M. Azarkin, I. Dremin, M. Kirakosyan, A. Leonidov, G. Mesyats, S. V. Rusakov, A. Vinogradov

**Skobeltsyn Institute of Nuclear Physics, Lomonosov Moscow State University, Moscow, Russia**
A. Belyaev, E. Boos, M. Dubinin[7], L. Dudko, A. Ershov, A. Gribushin, V. Klyukhin, O. Kodolova, I. Lokhtin, S. Obraztsov, M. Perfilov, S. Petrushanko, V. Savrin

**State Research Center of Russian Federation, Institute for High Energy Physics, Protvino, Russia**
I. Azhgirey, I. Bayshev, S. Bitioukov, V. Kachanov, A. Kalinin, D. Konstantinov, V. Krychkine, V. Petrov, R. Ryutin, A. Sobol, L. Tourtchanovitch, S. Troshin, N. Tyurin, A. Uzunian, A. Volkov

**University of Belgrade, Faculty of Physics and Vinca Institute of Nuclear Sciences, Belgrade, Serbia**
P. Adzic[37], M. Djordjevic, M. Ekmedzic, J. Milosevic

**Centro de Investigaciones Energéticas Medioambientales y Tecnológicas (CIEMAT), Madrid, Spain**
M. Aguilar-Benitez, J. Alcaraz Maestre, C. Battilana, E. Calvo, M. Cerrada, M. Chamizo Llatas[2], N. Colino, B. De La Cruz, A. Delgado Peris, D. Domínguez Vázquez, C. Fernandez Bedoya, J. P. Fernández Ramos, A. Ferrando, J. Flix, M. C. Fouz, P. Garcia-Abia, O. Gonzalez Lopez, S. Goy Lopez, J. M. Hernandez, M. I. Josa, G. Merino, E. Navarro De Martino, A. Pérez-Calero Yzquierdo, J. Puerta Pelayo, A. Quintario Olmeda, I. Redondo, L. Romero, M. S. Soares, C. Willmott

**Universidad Autónoma de Madrid, Madrid, Spain**
C. Albajar, J. F. de Trocóniz, M. Missiroli

**Universidad de Oviedo, Oviedo, Spain**
H. Brun, J. Cuevas, J. Fernandez Menendez, S. Folgueras, I. Gonzalez Caballero, L. Lloret Iglesias

**Instituto de Física de Cantabria (IFCA), CSIC-Universidad de Cantabria, Santander, Spain**
J. A. Brochero Cifuentes, I. J. Cabrillo, A. Calderon, J. Duarte Campderros, M. Fernandez, G. Gomez, J. Gonzalez Sanchez, A. Graziano, A. Lopez Virto, J. Marco, R. Marco, C. Martinez Rivero, F. Matorras, F. J. Munoz Sanchez, J. Piedra Gomez, T. Rodrigo, A. Y. Rodríguez-Marrero, A. Ruiz-Jimeno, L. Scodellaro, I. Vila, R. Vilar Cortabitarte

**CERN, European Organization for Nuclear Research, Geneva, Switzerland**
D. Abbaneo, E. Auffray, G. Auzinger, M. Bachtis, P. Baillon, A. H. Ball, D. Barney, A. Benaglia, J. Bendavid, L. Benhabib, J. F. Benitez, C. Bernet[8], G. Bianchi, P. Bloch, A. Bocci, A. Bonato, O. Bondu, C. Botta, H. Breuker, T. Camporesi, G. Cerminara, T. Christiansen, J. A. Coarasa Perez, S. Colafranceschi[38], M. D'Alfonso, D. d'Enterria, A. Dabrowski, A. David, F. De Guio, A. De Roeck, S. De Visscher, M. Dobson, N. Dupont-Sagorin, A. Elliott-Peisert, J. Eugster, G. Franzoni, W. Funk, M. Giffels, D. Gigi, K. Gill, D. Giordano, M. Girone, M. Giunta, F. Glege, R. Gomez-Reino Garrido, S. Gowdy, R. Guida, J. Hammer, M. Hansen, P. Harris, J. Hegeman, V. Innocente, P. Janot, E. Karavakis, K. Kousouris, K. Krajczar, P. Lecoq, C. Lourenço, N. Magini, L. Malgeri, M. Mannelli, L. Masetti, F. Meijers, S. Mersi, E. Meschi, F. Moortgat, M. Mulders, P. Musella, L. Orsini, E. Palencia Cortezon, L. Pape, E. Perez, L. Perrozzi, A. Petrilli, G. Petrucciani, A. Pfeiffer, M. Pierini, M. Pimiä, D. Piparo, M. Plagge, A. Racz, W. Reece, G. Rolandi[39], M. Rovere, H. Sakulin, F. Santanastasio, C. Schäfer, C. Schwick, S. Sekmen, A. Sharma, P. Siegrist, P. Silva, M. Simon, P. Sphicas[40], D. Spiga, J. Steggemann, B. Stieger, M. Stoye, D. Treille, A. Tsirou, G. I. Veres[21], J. R. Vlimant, H. K. Wöhri, W. D. Zeuner

**Paul Scherrer Institut, Villigen, Switzerland**
W. Bertl, K. Deiters, W. Erdmann, R. Horisberger, Q. Ingram, H. C. Kaestli, S. König, D. Kotlinski, U. Langenegger, D. Renker, T. Rohe

**Institute for Particle Physics, ETH Zurich, Zurich, Switzerland**
F. Bachmair, L. Bäni, L. Bianchini, P. Bortignon, M. A. Buchmann, B. Casal, N. Chanon, A. Deisher, G. Dissertori, M. Dittmar, M. Donegà, M. Dünser, P. Eller, C. Grab, D. Hits, W. Lustermann, B. Mangano, A. C. Marini, P. Martinez Ruiz del Arbol, D. Meister, N. Mohr, C. Nägeli[41], P. Nef, F. Nessi-Tedaldi, F. Pandolfi, F. Pauss, M. Peruzzi, M. Quittnat, L. Rebane, F. J. Ronga, M. Rossini, A. Starodumov[42], M. Takahashi, K. Theofilatos, R. Wallny, H. A. Weber

**Universität Zürich, Zurich, Switzerland**
C. Amsler[43], M. F. Canelli, V. Chiochia, A. De Cosa, C. Favaro, A. Hinzmann, T. Hreus, M. Ivova Rikova, B. Kilminster, B. Millan Mejias, J. Ngadiuba, P. Robmann, H. Snoek, S. Taroni, M. Verzetti, Y. Yang

**National Central University, Chung-Li, Taiwan**
M. Cardaci, K. H. Chen, C. Ferro, C. M. Kuo, S. W. Li, W. Lin, Y. J. Lu, R. Volpe, S. S. Yu

**National Taiwan University (NTU), Taipei, Taiwan**
P. Bartalini, P. Chang, Y. H. Chang, Y. W. Chang, Y. Chao, K. F. Chen, P. H. Chen, C. Dietz, U. Grundler, W.-S. Hou, Y. Hsiung, K. Y. Kao, Y. J. Lei, Y. F. Liu, R.-S. Lu, D. Majumder, E. Petrakou, X. Shi, J. G. Shiu, Y. M. Tzeng, M. Wang, R. Wilken

**Chulalongkorn University, Bangkok, Thailand**
B. Asavapibhop, N. Suwonjandee

**Cukurova University, Adana, Turkey**
A. Adiguzel, M. N. Bakirci[44], S. Cerci[45], C. Dozen, I. Dumanoglu, E. Eskut, S. Girgis, G. Gokbulut, E. Gurpinar, I. Hos, E. E. Kangal, A. Kayis Topaksu, G. Onengut[46], K. Ozdemir, S. Ozturk[44], A. Polatoz, K. Sogut[47], D. Sunar Cerci[45], B. Tali[45], H. Topakli[44], M. Vergili

**Physics Department, Middle East Technical University, Ankara, Turkey**
I. V. Akin, T. Aliev, B. Bilin, S. Bilmis, M. Deniz, H. Gamsizkan, A. M. Guler, G. Karapinar[48], K. Ocalan, A. Ozpineci, M. Serin, R. Sever, U. E. Surat, M. Yalvac, M. Zeyrek

**Bogazici University, Istanbul, Turkey**
E. Gülmez, B. Isildak[49], M. Kaya[50], O. Kaya[50], S. Ozkorucuklu[51]

**Istanbul Technical University, Istanbul, Turkey**
H. Bahtiyar[52], E. Barlas, K. Cankocak, Y. O. Günaydin[53], F. I. Vardarlı, M. Yücel

**National Scientific Center, Kharkov Institute of Physics and Technology, Kharkiv, Ukraine**
L. Levchuk, P. Sorokin

**University of Bristol, Bristol, UK**
J. J. Brooke, E. Clement, D. Cussans, H. Flacher, R. Frazier, J. Goldstein, M. Grimes, G. P. Heath, H. F. Heath, J. Jacob, L. Kreczko, C. Lucas, Z. Meng, D. M. Newbold[54], S. Paramesvaran, A. Poll, S. Senkin, V. J. Smith, T. Williams

**Rutherford Appleton Laboratory, Didcot, UK**
K. W. Bell, A. Belyaev[55], C. Brew, R. M. Brown, D. J. A. Cockerill, J. A. Coughlan, K. Harder, S. Harper, J. Ilic, E. Olaiya, D. Petyt, C. H. Shepherd-Themistocleous, A. Thea, I. R. Tomalin, W. J. Womersley, S. D. Worm

**Imperial College, London, UK**
M. Baber, R. Bainbridge, O. Buchmuller, D. Burton, D. Colling, N. Cripps, M. Cutajar, P. Dauncey, G. Davies, M. Della Negra, W. Ferguson, J. Fulcher, D. Futyan, A. Gilbert, A. Guneratne Bryer, G. Hall, Z. Hatherell, J. Hays, G. Iles, M. Jarvis, G. Karapostoli, M. Kenzie, R. Lane, R. Lucas[54], L. Lyons, A.-M. Magnan, J. Marrouche, B. Mathias, R. Nandi, J. Nash, A. Nikitenko[42], J. Pela, M. Pesaresi, K. Petridis, M. Pioppi[56], D. M. Raymond, S. Rogerson, A. Rose, C. Seez, P. Sharp†, A. Sparrow, A. Tapper, M. Vazquez Acosta, T. Virdee, S. Wakefield, N. Wardle

**Brunel University, Uxbridge, UK**
J. E. Cole, P. R. Hobson, A. Khan, P. Kyberd, D. Leggat, D. Leslie, W. Martin, I. D. Reid, P. Symonds, L. Teodorescu, M. Turner

**Baylor University, Waco, USA**
J. Dittmann, K. Hatakeyama, A. Kasmi, H. Liu, T. Scarborough

**The University of Alabama, Tuscaloosa, USA**
O. Charaf, S. I. Cooper, C. Henderson, P. Rumerio

**Boston University, Boston, USA**
A. Avetisyan, T. Bose, C. Fantasia, A. Heister, P. Lawson, D. Lazic, C. Richardson, J. Rohlf, D. Sperka, J. St. John, L. Sulak

**Brown University, Providence, USA**
J. Alimena, S. Bhattacharya, G. Christopher, D. Cutts, Z. Demiragli, A. Ferapontov, A. Garabedian, U. Heintz, S. Jabeen, G. Kukartsev, E. Laird, G. Landsberg, M. Luk, M. Narain, M. Segala, T. Sinthuprasith, T. Speer, J. Swanson

**University of California, Davis, USA**
R. Breedon, G. Breto, M. Calderon De La Barca Sanchez, S. Chauhan, M. Chertok, J. Conway, R. Conway, P. T. Cox, R. Erbacher, M. Gardner, W. Ko, A. Kopecky, R. Lander, T. Miceli, M. Mulhearn, D. Pellett, J. Pilot, F. Ricci-Tam, B. Rutherford, M. Searle, S. Shalhout, J. Smith, M. Squires, M. Tripathi, S. Wilbur, R. Yohay

**University of California, Los Angeles, USA**
V. Andreev, D. Cline, R. Cousins, S. Erhan, P. Everaerts, C. Farrell, M. Felcini, J. Hauser, M. Ignatenko, C. Jarvis, G. Rakness, E. Takasugi, V. Valuev, M. Weber

**University of California, Riverside, Riverside, USA**
J. Babb, R. Clare, J. Ellison, J. W. Gary, G. Hanson, J. Heilman, P. Jandir, F. Lacroix, H. Liu, O. R. Long, A. Luthra, M. Malberti, H. Nguyen, A. Shrinivas, J. Sturdy, S. Sumowidagdo, S. Wimpenny

**University of California, San Diego, La Jolla, USA**
W. Andrews, J. G. Branson, G. B. Cerati, S. Cittolin, R. T. D'Agnolo, D. Evans, A. Holzner, R. Kelley, D. Kovalskyi, M. Lebourgeois, J. Letts, I. Macneill, S. Padhi, C. Palmer, M. Pieri, M. Sani, V. Sharma, S. Simon, E. Sudano, M. Tadel, Y. Tu, A. Vartak, S. Wasserbaech[57], F. Würthwein, A. Yagil, J. Yoo

**University of California, Santa Barbara, Santa Barbara, USA**
D. Barge, J. Bradmiller-Feld, C. Campagnari, T. Danielson, A. Dishaw, K. Flowers, M. Franco Sevilla, P. Geffert, C. George, F. Golf, J. Incandela, C. Justus, R. Magaña Villalba, N. Mccoll, V. Pavlunin, J. Richman, R. Rossin, D. Stuart, W. To, C. West

**California Institute of Technology, Pasadena, USA**
A. Apresyan, A. Bornheim, J. Bunn, Y. Chen, E. Di Marco, J. Duarte, D. Kcira, A. Mott, H. B. Newman, C. Pena, C. Rogan, M. Spiropulu, V. Timciuc, R. Wilkinson, S. Xie, R. Y. Zhu

**Carnegie Mellon University, Pittsburgh, USA**
V. Azzolini, A. Calamba, R. Carroll, T. Ferguson, Y. Iiyama, D. W. Jang, M. Paulini, J. Russ, H. Vogel, I. Vorobiev

**University of Colorado at Boulder, Boulder, USA**
J. P. Cumalat, B. R. Drell, W. T. Ford, A. Gaz, E. Luiggi Lopez, U. Nauenberg, J. G. Smith, K. Stenson, K. A. Ulmer, S. R. Wagner

**Cornell University, Ithaca, USA**
J. Alexander, A. Chatterjee, J. Chu, N. Eggert, L. K. Gibbons, W. Hopkins, A. Khukhunaishvili, B. Kreis, N. Mirman, G. Nicolas Kaufman, J. R. Patterson, A. Ryd, E. Salvati, W. Sun, W. D. Teo, J. Thom, J. Thompson, J. Tucker, Y. Weng, L. Winstrom, P. Wittich

**Fairfield University, Fairfield, USA**
D. Winn

**Fermi National Accelerator Laboratory, Batavia, USA**
S. Abdullin, M. Albrow, J. Anderson, G. Apollinari, L. A. T. Bauerdick, A. Beretvas, J. Berryhill, P. C. Bhat, K. Burkett, J. N. Butler, V. Chetluru, H. W. K. Cheung, F. Chlebana, S. Cihangir, V. D. Elvira, I. Fisk, J. Freeman, Y. Gao, E. Gottschalk, L. Gray, D. Green, S. Grünendahl, O. Gutsche, D. Hare, R. M. Harris, J. Hirschauer, B. Hooberman, S. Jindariani, M. Johnson, U. Joshi, K. Kaadze, B. Klima, S. Kwan, J. Linacre, D. Lincoln, R. Lipton, T. Liu, J. Lykken, K. Maeshima, J. M. Marraffino, V. I. Martinez Outschoorn, S. Maruyama, D. Mason, P. McBride, K. Mishra, S. Mrenna, Y. Musienko[35], S. Nahn, C. Newman-Holmes, V. O'Dell, O. Prokofyev, N. Ratnikova, E. Sexton-Kennedy, S. Sharma, A. Soha, W. J. Spalding, L. Spiegel, L. Taylor, S. Tkaczyk, N. V. Tran, L. Uplegger, E. W. Vaandering, R. Vidal, A. Whitbeck, J. Whitmore, W. Wu, F. Yang, J. C. Yun

**University of Florida, Gainesville, USA**
D. Acosta, P. Avery, D. Bourilkov, T. Cheng, S. Das, M. De Gruttola, G. P. Di Giovanni, D. Dobur, R. D. Field, M. Fisher, Y. Fu, I. K. Furic, J. Hugon, B. Kim, J. Konigsberg, A. Korytov, A. Kropivnitskaya, T. Kypreos, J. F. Low, K. Matchev, P. Milenovic[58], G. Mitselmakher, L. Muniz, A. Rinkevicius, L. Shchutska, N. Skhirtladze, M. Snowball, J. Yelton, M. Zakaria

**Florida International University, Miami, USA**
V. Gaultney, S. Hewamanage, S. Linn, P. Markowitz, G. Martinez, J. L. Rodriguez

**Florida State University, Tallahassee, USA**
T. Adams, A. Askew, J. Bochenek, J. Chen, B. Diamond, J. Haas, S. Hagopian, V. Hagopian, K. F. Johnson, H. Prosper, V. Veeraraghavan, M. Weinberg

**Florida Institute of Technology, Melbourne, USA**
M. M. Baarmand, B. Dorney, M. Hohlmann, H. Kalakhety, F. Yumiceva

**University of Illinois at Chicago (UIC), Chicago, USA**
M. R. Adams, L. Apanasevich, V. E. Bazterra, R. R. Betts, I. Bucinskaite, R. Cavanaugh, O. Evdokimov, L. Gauthier, C. E. Gerber, D. J. Hofman, S. Khalatyan, P. Kurt, D. H. Moon, C. O'Brien, C. Silkworth, P. Turner, N. Varelas

**The University of Iowa, Iowa City, USA**
U. Akgun, E. A. Albayrak[52], B. Bilki[59], W. Clarida, K. Dilsiz, F. Duru, M. Haytmyradov, J.-P. Merlo, H. Mermerkaya[60], A. Mestvirishvili, A. Moeller, J. Nachtman, H. Ogul, Y. Onel, F. Ozok[52], A. Penzo, R. Rahmat, S. Sen, P. Tan, E. Tiras, J. Wetzel, T. Yetkin[61], K. Yi

**Johns Hopkins University, Baltimore, USA**
B. A. Barnett, B. Blumenfeld, S. Bolognesi, D. Fehling, A. V. Gritsan, P. Maksimovic, C. Martin, M. Swartz

**The University of Kansas, Lawrence, USA**
P. Baringer, A. Bean, G. Benelli, J. Gray, R. P. Kenny III, M. Murray, D. Noonan, S. Sanders, J. Sekaric, R. Stringer, Q. Wang, J. S. Wood

**Kansas State University, Manhattan, USA**
A. F. Barfuss, I. Chakaberia, A. Ivanov, S. Khalil, M. Makouski, Y. Maravin, L. K. Saini, S. Shrestha, I. Svintradze

**Lawrence Livermore National Laboratory, Livermore, USA**
J. Gronberg, D. Lange, F. Rebassoo, D. Wright

**University of Maryland, College Park, USA**
A. Baden, B. Calvert, S. C. Eno, J. A. Gomez, N. J. Hadley, R. G. Kellogg, T. Kolberg, Y. Lu, M. Marionneau, A. C. Mignerey, K. Pedro, A. Skuja, J. Temple, M. B. Tonjes, S. C. Tonwar

**Massachusetts Institute of Technology, Cambridge, USA**
A. Apyan, R. Barbieri, G. Bauer, W. Busza, I. A. Cali, M. Chan, L. Di Matteo, V. Dutta, G. Gomez Ceballos, M. Goncharov, D. Gulhan, M. Klute, Y. S. Lai, Y.-J. Lee, A. Levin, P. D. Luckey, T. Ma, C. Paus, D. Ralph, C. Roland, G. Roland, G. S. F. Stephans, F. Stöckli, K. Sumorok, D. Velicanu, J. Veverka, B. Wyslouch, M. Yang, A. S. Yoon, M. Zanetti, V. Zhukova

**University of Minnesota, Minneapolis, USA**
B. Dahmes, A. De Benedetti, A. Gude, S. C. Kao, K. Klapoetke, Y. Kubota, J. Mans, N. Pastika, R. Rusack, A. Singovsky, N. Tambe, J. Turkewitz

**University of Mississippi, Oxford, USA**
J. G. Acosta, L. M. Cremaldi, R. Kroeger, S. Oliveros, L. Perera, D. A. Sanders, D. Summers

**University of Nebraska-Lincoln, Lincoln, USA**
E. Avdeeva, K. Bloom, S. Bose, D. R. Claes, A. Dominguez, R. Gonzalez Suarez, J. Keller, D. Knowlton, I. Kravchenko, J. Lazo-Flores, S. Malik, F. Meier, G. R. Snow

**State University of New York at Buffalo, Buffalo, USA**
J. Dolen, A. Godshalk, I. Iashvili, S. Jain, A. Kharchilava, A. Kumar, S. Rappoccio

**Northeastern University, Boston, USA**
G. Alverson, E. Barberis, D. Baumgartel, M. Chasco, J. Haley, A. Massironi, D. Nash, T. Orimoto, D. Trocino, D. Wood, J. Zhang

**Northwestern University, Evanston, USA**
A. Anastassov, K. A. Hahn, A. Kubik, L. Lusito, N. Mucia, N. Odell, B. Pollack, A. Pozdnyakov, M. Schmitt, S. Stoynev, K. Sung, M. Velasco, S. Won

**University of Notre Dame, Notre Dame, USA**
D. Berry, A. Brinkerhoff, K. M. Chan, A. Drozdetskiy, M. Hildreth, C. Jessop, D. J. Karmgard, N. Kellams, J. Kolb, K. Lannon, W. Luo, S. Lynch, N. Marinelli, D. M. Morse, T. Pearson, M. Planer, R. Ruchti, J. Slaunwhite, N. Valls, M. Wayne, M. Wolf, A. Woodard

**The Ohio State University, Columbus, USA**
L. Antonelli, B. Bylsma, L. S. Durkin, S. Flowers, C. Hill, R. Hughes, K. Kotov, T. Y. Ling, D. Puigh, M. Rodenburg, G. Smith, C. Vuosalo, B. L. Winer, H. Wolfe, H. W. Wulsin

**Princeton University, Princeton, USA**
E. Berry, P. Elmer, V. Halyo, P. Hebda, A. Hunt, P. Jindal, S. A. Koay, P. Lujan, D. Marlow, T. Medvedeva, M. Mooney, J. Olsen, P. Piroué, X. Quan, A. Raval, H. Saka, D. Stickland, C. Tully, J. S. Werner, S. C. Zenz, A. Zuranski

**University of Puerto Rico, Mayaguez, USA**
E. Brownson, A. Lopez, H. Mendez, J. E. Ramirez Vargas

**Purdue University, West Lafayette, USA**
E. Alagoz, D. Benedetti, G. Bolla, D. Bortoletto, M. De Mattia, A. Everett, Z. Hu, M. K. Jha, M. Jones, K. Jung, M. Kress, N. Leonardo, D. Lopes Pegna, V. Maroussov, P. Merkel, D. H. Miller, N. Neumeister, B. C. Radburn-Smith, I. Shipsey, D. Silvers, A. Svyatkovskiy, F. Wang, W. Xie, L. Xu, H. D. Yoo, J. Zablocki, Y. Zheng

**Purdue University Calumet, Hammond, USA**
N. Parashar

**Rice University, Houston, USA**
A. Adair, B. Akgun, K. M. Ecklund, F. J. M. Geurts, W. Li, B. Michlin, B. P. Padley, R. Redjimi, J. Roberts, J. Zabel

**University of Rochester, Rochester, USA**
B. Betchart, A. Bodek, R. Covarelli, P. de Barbaro, R. Demina, Y. Eshaq, T. Ferbel, A. Garcia-Bellido, P. Goldenzweig, J. Han, A. Harel, D. C. Miner, G. Petrillo, D. Vishnevskiy, M. Zielinski

**The Rockefeller University, New York, USA**
A. Bhatti, R. Ciesielski, L. Demortier, K. Goulianos, G. Lungu, S. Malik, C. Mesropian

**Rutgers, The State University of New Jersey, Piscataway, USA**
S. Arora, A. Barker, J. P. Chou, C. Contreras-Campana, E. Contreras-Campana, D. Duggan, D. Ferencek, Y. Gershtein, R. Gray, E. Halkiadakis, D. Hidas, A. Lath, S. Panwalkar, M. Park, R. Patel, V. Rekovic, J. Robles, S. Salur, S. Schnetzer, C. Seitz, S. Somalwar, R. Stone, S. Thomas, P. Thomassen, M. Walker

**University of Tennessee, Knoxville, USA**
K. Rose, S. Spanier, Z. C. Yang, A. York

**Texas A&M University, College Station, USA**
O. Bouhali[62], R. Eusebi, W. Flanagan, J. Gilmore, T. Kamon[63], V. Khotilovich, V. Krutelyov, R. Montalvo, I. Osipenkov, Y. Pakhotin, A. Perloff, J. Roe, A. Rose, A. Safonov, T. Sakuma, I. Suarez, A. Tatarinov, D. Toback

**Texas Tech University, Lubbock, USA**
N. Akchurin, C. Cowden, J. Damgov, C. Dragoiu, P. R. Dudero, J. Faulkner, K. Kovitanggoon, S. Kunori, S. W. Lee, T. Libeiro, I. Volobouev

**Vanderbilt University, Nashville, USA**
E. Appelt, A. G. Delannoy, S. Greene, A. Gurrola, W. Johns, C. Maguire, Y. Mao, A. Melo, M. Sharma, P. Sheldon, B. Snook, S. Tuo, J. Velkovska

**University of Virginia, Charlottesville, USA**
M. W. Arenton, S. Boutle, B. Cox, B. Francis, J. Goodell, R. Hirosky, A. Ledovskoy, H. Li, C. Lin, C. Neu, J. Wood

**Wayne State University, Detroit, USA**
S. Gollapinni, R. Harr, P. E. Karchin, C. Kottachchi Kankanamge Don, P. Lamichhane

**University of Wisconsin, Madison, USA**
D. A. Belknap, L. Borrello, D. Carlsmith, M. Cepeda, S. Dasu, S. Duric, E. Friis, M. Grothe, R. Hall-Wilton, M. Herndon, A. Hervé, P. Klabbers, J. Klukas, A. Lanaro, C. Lazaridis, A. Levine, R. Loveless, A. Mohapatra, I. Ojalvo, T. Perry, G. A. Pierro, G. Polese, I. Ross, T. Sarangi, A. Savin, W. H. Smith, N. Woods

† **Deceased**

1: Also at Vienna University of Technology, Vienna, Austria
2: Also at CERN, European Organization for Nuclear Research, Geneva, Switzerland
3: Also at Institut Pluridisciplinaire Hubert Curien, Université de Strasbourg, Université de Haute Alsace Mulhouse, CNRS/IN2P3, Strasbourg, France
4: Also at National Institute of Chemical Physics and Biophysics, Tallinn, Estonia
5: Also at Skobeltsyn Institute of Nuclear Physics, Lomonosov Moscow State University, Moscow, Russia
6: Also at Universidade Estadual de Campinas, Campinas, Brazil
7: Also at California Institute of Technology, Pasadena, USA
8: Also at Laboratoire Leprince-Ringuet, Ecole Polytechnique, IN2P3-CNRS, Palaiseau, France
9: Also at Suez University, Suez, Egypt
10: Also at Zewail City of Science and Technology, Zewail, Egypt
11: Also at Cairo University, Cairo, Egypt
12: Also at Fayoum University, El-Fayoum, Egypt
13: Also at Helwan University, Cairo, Egypt
14: Also at British University in Egypt, Cairo, Egypt
15: Now at Ain Shams University, Cairo, Egypt
16: Also at Université de Haute Alsace, Mulhouse, France
17: Also at Joint Institute for Nuclear Research, Dubna, Russia
18: Also at Brandenburg University of Technology, Cottbus, Germany
19: Also at The University of Kansas, Lawrence, USA
20: Also at Institute of Nuclear Research ATOMKI, Debrecen, Hungary
21: Also at Eötvös Loránd University, Budapest, Hungary
22: Also at Tata Institute of Fundamental Research-HECR, Mumbai, India
23: Now at King Abdulaziz University, Jeddah, Saudi Arabia
24: Also at University of Visva-Bharati, Santiniketan, India
25: Also at University of Ruhuna, Matara, Sri Lanka
26: Also at Isfahan University of Technology, Isfahan, Iran
27: Also at Sharif University of Technology, Tehran, Iran
28: Also at Plasma Physics Research Center, Science and Research Branch, Islamic Azad University, Tehran, Iran
29: Also at Laboratori Nazionali di Legnaro dell'INFN, Legnaro, Italy
30: Also at Università degli Studi di Siena, Siena, Italy
31: Also at Centre National de la Recherche Scientifique (CNRS)-IN2P3, Paris, France
32: Also at Purdue University, West Lafayette, USA
33: Also at Universidad Michoacana de San Nicolas de Hidalgo, Morelia, Mexico
34: Also at National Centre for Nuclear Research, Swierk, Poland
35: Also at Institute for Nuclear Research, Moscow, Russia
36: Also at St. Petersburg State Polytechnical University, St. Petersburg, Russia
37: Also at Faculty of Physics, University of Belgrade, Belgrade, Serbia
38: Also at Facoltà Ingegneria, Università di Roma, Rome, Italy
39: Also at Scuola Normale e Sezione dell'INFN, Pisa, Italy
40: Also at University of Athens, Athens, Greece
41: Also at Paul Scherrer Institut, Villigen, Switzerland
42: Also at Institute for Theoretical and Experimental Physics, Moscow, Russia
43: Also at Albert Einstein Center for Fundamental Physics, Bern, Switzerland
44: Also at Gaziosmanpasa University, Tokat, Turkey
45: Also at Adiyaman University, Adiyaman, Turkey
46: Also at Cag University, Mersin, Turkey

47: Also at Mersin University, Mersin, Turkey
48: Also at Izmir Institute of Technology, Izmir, Turkey
49: Also at Ozyegin University, Istanbul, Turkey
50: Also at Kafkas University, Kars, Turkey
51: Also at Istanbul University, Faculty of Science, Istanbul, Turkey
52: Also at Mimar Sinan University, Istanbul, Istanbul, Turkey
53: Also at Kahramanmaras Sütcü Imam University, Kahramanmaras, Turkey
54: Also at Rutherford Appleton Laboratory, Didcot, UK
55: Also at School of Physics and Astronomy, University of Southampton, Southampton, UK
56: Also at INFN Sezione di Perugia; Università di Perugia, Perugia, Italy
57: Also at Utah Valley University, Orem, USA
58: Also at University of Belgrade, Faculty of Physics and Vinca Institute of Nuclear Sciences, Belgrade, Serbia
59: Also at Argonne National Laboratory, Argonne, USA
60: Also at Erzincan University, Erzincan, Turkey
61: Also at Yildiz Technical University, Istanbul, Turkey
62: Also at Texas A&M University at Qatar, Doha, Qatar
63: Also at Kyungpook National University, Taegu, Korea